Bioorganic Chemistry 88 (2019) 102929

Contents lists available at ScienceDirect

Bioorganic Chemistry

journal homepage: www.elsevier.com/locate/bioorg

Design, synthesis, anticancer evaluation, molecular docking and cell cycle analysis of 3-methyl-4,7-dihydropyrazolo[1,5-*a*]pyrimidine derivatives as potent histone lysine demethylases (KDM) inhibitors and apoptosis inducers

Nadia Hanafy Metwally*, Mona Said Mohamed, Eman Ali Ragb

Department of Chemistry, Faculty of Science, Cairo University, Giza, Egypt

ARTICLE INFO

Keywords:
Pyrazolo[1,5-*a*]pyrimidines
Cytotoxic activity
Histone lysine demethylases (KDM) inhibitor
Cell cycle
Apoptotic effect
Lipinsk's rule
Molecular docking and bioinformatics studies

ABSTRACT

A novel series of pyrazolo[1,5-*a*]pyrimidines were synthesized and proved by their spectral and elemental analysis, some elected of the newly synthesized compounds were examined for their cytotoxic activity employing MTT assay on two cancer cell lines (Breast and Hela cancers). Compounds **5**, **7e** and **7i** showed the higher cytotoxicity against two cancer cell lines with (IC_{50} = 13.91 ± 1.4 and 22.37 ± 1.8 μM/L), (IC_{50} = 6.56 ± 0.5 and 8.72 ± 0.9 μM/L) and (IC_{50} = 4.17 ± 0.2 and 5.57 ± 0.4 μM/L) for two cancer cell lines breast and hela respectively, using doxorubicin as a reference drug. The most potent cytotoxic active compounds **5**, **7e** and **7i** presented inhibitory activity against KDM (histone lysine demethylases) with IC_{50} = 4.05, 1.91 and 2.31 μM, respectively. The most potent KDM inhibitor **7e** (IC_{50} = 1.91 μM) showed to cause cell cycle arrest at G2/M phase by 4 folds than control and induce total apoptotic effect by 10 folds more than control. In silico studies performed on the more potent cytotoxic active compounds **5**, **7e** and **7i** included lipinisk's rule of five. Moreover, molecular docking study was utilized to explore the binding mode of the most active compounds to the target enzyme (PDB-ID: 5IVE). Also, some bioinformatics studies were carried out for compounds **7e** and **7i** using Swiss ADME (Swiss Institute of bioinformatics 2018).

1. Introduction

Cancer, the rapid uncontrolled growth of abnormal cells [1] and is the second leading cause of death after cardiovascular diseases in the terms of morbidity and mortality according to world health organization (WHO) [2]. Cancers that affect women are divided into six types such as cervical, endometrial, fallopian tube, breast, ovarian and vaginal cancers: breast and cervical cancers are the most common types occurring, considered as the second and fourth leading cause of cancer death. Several agents directed against critical breast cancer enhancing proteins are currently being developed such as inhibitors against the poly(ADP-ribose) polymerase [3], cyclin dependent kinases 4 and 6 (CDK4/6) [4], as well as against the KDM4 enzymes [5]. Moreover, some inhibitors used against cervical cancer such as dynamin 2 which plays an important role in vascular endothelial growth factor (VEGF)-mediated angiogenesis [6].

Histones are highly alkaline proteins in eukaryotic cells; DNA is packed together with histone proteins in a highly organized form called chromatin. Methylation of histone lysine plays an important role in maintaining the structure of chromatin and regulation of transcription. Disturbance of histone methylation is a good factor for cancer development and progression [7,8]. The maintaining of histone lysine methylation depend on two enzyme families histone lysine methyl transferase (KMTs) and histone lysine demethylases (KDMs) [9]. Shi et al. discovered two families of KDM [10]. One is specific-lysine demethylase (LSD) that belongs to flavin adenine dinucleotide (FAD)-dependent monoamine oxidase and the other KDMs belong to Jumonji domain containing lysine demethylases (JmjC KDMs) which divided into six subfamilies (KDM2-7) with different demethylated catalysis activities. KDM4A and other members in KDM4 subfamily are catalyze the demethylation of histone H3 subunit lysine9 tri-/di-methylated mark ($H3K9me_{3/2}$) [11]. Additionally, histone lysine demethylases (KDM5A-D) family members are responsible for removing methyl group of (trimethylated) lysine 4 on histone 3(H3K4me3). In addition, KDM5 family found to play a role as oncogenic driver (molecules which cause the formation or support the progression of cancer). It has been shown that KDM5A and KDM5B are required for cancer cell survival, this is due to an increase in gene expression in a number of human cancer cells such as breast (MCF-7) [12]. Therefore, KDM5 inhibitors considered as drug used in cancer treatment.

* Corresponding author.
E-mail address: nhmmohamed@yahoo.com (N.H. Metwally).

https://doi.org/10.1016/j.bioorg.2019.102929
Received 16 December 2018; Received in revised form 11 April 2019; Accepted 15 April 2019
Available online 16 April 2019

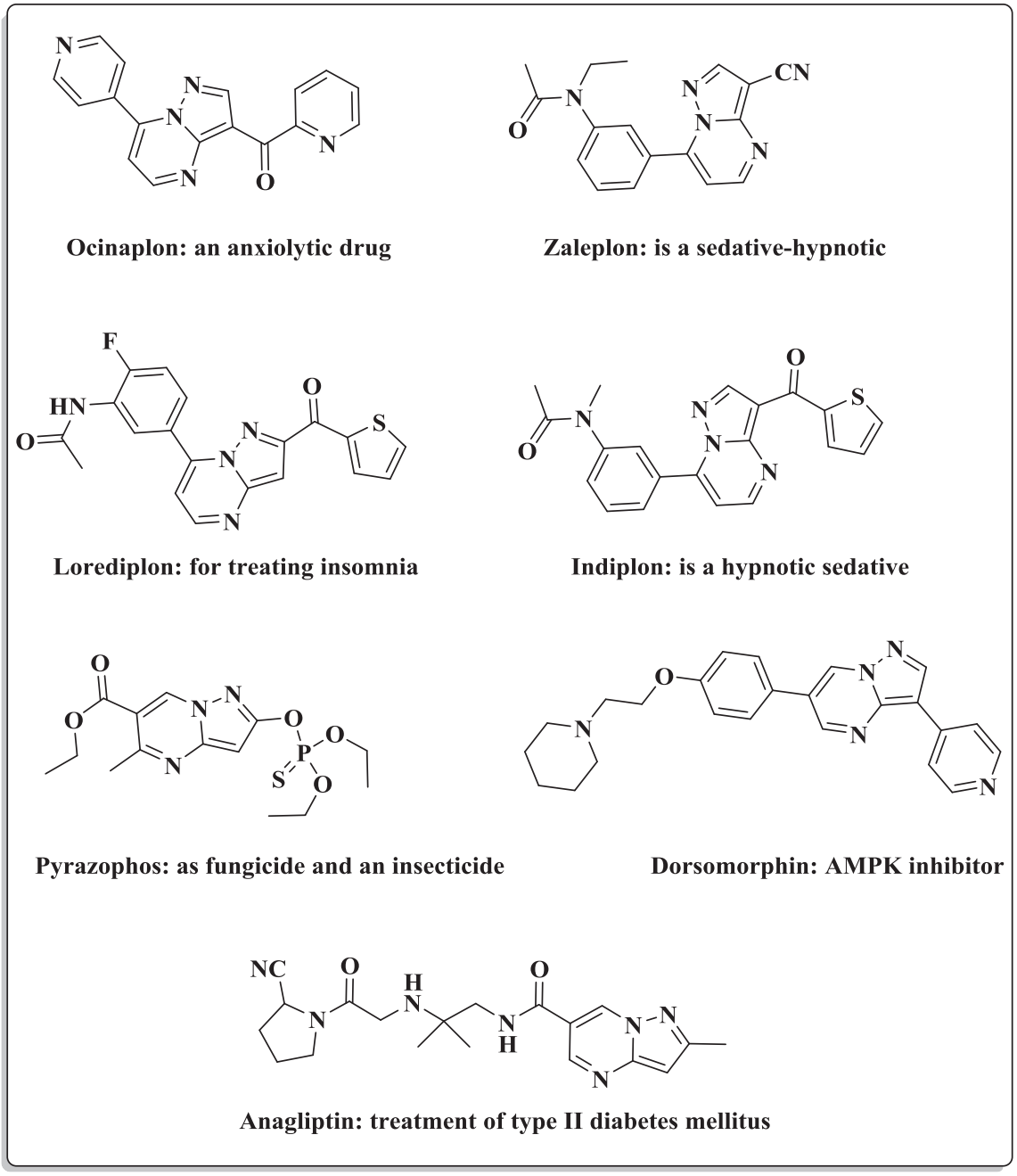

Fig. 1. Marketed drug based on pyrazolo[1,5-*a*]pyrimidine.

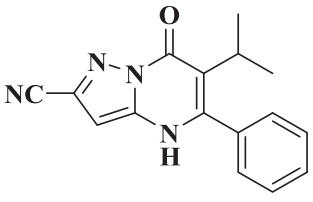

CPI-455

IC_{50} = 0.01 M

KDM5A

Fig. 2. CPI-455 as inhibitor of KDM5A.

On the other hand, pyrazolo[1,5-*a*]pyrimidine scaffold considered as an important class of heterocyclic compounds in the area of drug design as they are analogs to purine ring with a variety of medicinal applications as anticancer [13], HCV inhibitors [14], anxiolytic [15], positron emission tomography (PET) tumor imaging agents [16], HIV reverse transcriptase inhibitors [17] and kinase inhibitors [18]. Pyrazolo[1,5-*a*]pyrimidine (core moiety) considered as important marketed drugs like loredipion and pyrazophos [19], ocinaplon [20], dorsomorphin [21], anagliptin [22], zaleplon and indiplon [23] as presented in Fig. 1.

Moreover, it has been reported that 6-isopropyl-7-oxo-5-phenyl-4,7-dihydropyrazolo[1,5-*a*]pyrimidine-2-carbonitrile (CPI-455) is identified as an inhibitor of KDM5A through a high-throughput screening (HTS) assay against KDM4C JmjC domain and subsequent structural modification work [24,25]. It exhibited good potency toward KDM5A with IC_{50} = 0.02 μM. Also, compound CPI-455 could specifically

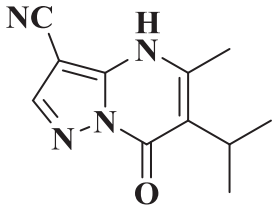

Fig. 3. The native ligand of the protein active site (5IVE).

increase H3K4me$_{3/2}$ in a dose-dependent manner in PC9, M14 and SKBR3 cells (Fig. 2).

Thus, in view of the above mention and in continuation of our work to synthesize bioactive heterocyclic ring systems of interest biological activity [26–30], we report herein the synthesize of some novel pyrazolo[1,5-*a*]pyrimidines (Fig. 4) which investigated in *vitro* cytotoxic activity against two human cancer cell lines breast (MCF-7) and HeL a promising to be KDM5A (Jumonji domain) histone lysine demethylase inhibitors and used in treatment of breast and HeLa cancer cells which their structure like the native ligand of protein active site 5IVE as shown in Fig. 3.

2. Results and discussion

2.1. Chemistry

Cyclocondesation of 5-amino-3-cyanomethyl-1*H*-pyrazole-4-carbonitrile (**1**) with acetoacetanilide (**2**) in *N*,*N*-dimethylformamide containing a few drops of glacial acetic acid produced the isolated product **5** (Scheme 1). The IR spectrum of the isolated product **5** presented absorption bands at ν_{max} 3152, 2227 and 1671 cm^{-1} corresponding to NH, 2CN and CO groups, respectively. The ^{1}H NMR spectrum of **5** not appeared a multiplet signals at δ near ~7.0–8.0 ppm corresponding to aryl protons and appeared three singlet signals at δ = 2.38, 4.36 and 5.87 ppm owing to methyl (CH_3), methylene ($C\underline{H}_2CN$), and pyrimidine protons along with a D_2O exchangeable signal at δ = 13.35 ppm due to NH proton. In addition, mass spectrum of **5** indicated a correct molecular ion peak at *m/z* = 213 (M^+) accordance with the molecular formula $C_{10}H_7N_5O$. According to our results, we have postulated a route for the formation of compound **5**. The reaction mechanism proceeds through the nucleophilic attack of the exo-NH_2 function from 5-aminopyrazoles **1** on the carbonyl group of acetoacetanilide **2**, by releasing water molecule, to form intermediate imine **A**, followed by intramolecular cyclization occurs by a nucleophilic attack of the NH pyrazole ring on the other carbonyl group to form an intermediate adduct **B** followed by the elimination of aniline yields **5** and ruled out the formation of each of compound **3** and **4** (Scheme 1).

Condensation of compound **5** with various aromatic aldehydes **6a-i** in refluxing *N*,*N*-dimethylformamide containing few drops of piperidine afforded the corresponding arylidene derivatives **7a-i** (Scheme 2). The IR spectrum of the isolated product **7e** as representative example of the prepared series showed absorption bands at ν_{max} 3410, 2214 and 1628 cm^{-1} corresponding to NH, two CN and CO groups, respectively. The ^{1}H NMR spectrum of **7e** revealed the presence of a singlet signal at δ = 5.56 ppm assigned for pyrimidine proton, in addition to aryl protons at δ = 6.81–7.95 ppm. Also, a singlet signal at δ = 8.09 ppm attributable to vinylic proton. The elemental analyses with mass spectrum of **7e** showed a correct molecular ion peak at *m/z* = 291 (M^+, 1.3%) which affirmed the molecular formula $C_{15}H_9N_5O_2$ (Scheme 2).

Moreover, compounds **5** condensed with *o*-hydroxybenzaldehydes **8a,b** under the same reaction conditions afforded in each case, red solid of melting point above 300 °C **10a,b** (Scheme 3). The IR spectrum of compound **10a** exhibited absorption bands at ν_{max} 3431, 2212 and 1628 cm^{-1} due to NH, CN and CO groups, respectively. It's ^{1}H NMR spectrum clarified the presence of two D_2O-exchangeable signals at δ = 9.11 and 10.21 ppm assigned to two NH protons. Refluxing the compounds **10a,b** in sodium ethoxide solution gave products **11a,b**. The structure of the isolated products **11a,b** was deduced from correct analytical and spectral data. The IR spectrum of **11a** showed disappearance of an absorption band corresponding to nitrile group near to ν_{max} ~2200 cm^{-1} and instead revealed an absorption band at ν_{max} 3209 cm^{-1} due to NH group.

On the other hand, refluxing of compounds **5** with indoline-2,3-dione **12** under the same reaction conditions afforded a brown solid **14** of melting point above 300 °C (Scheme 4). The IR spectrum of compound **14** appeared absorption bands at ν_{max} 3418, 3209, 2214 and 1656 cm^{-1} relative to 2NH, CN and CO groups, respectively. It's ^{1}H NMR also, indicated the presence of two D_2O-exchangeable signals at δ = 8.42 and 8.62 ppm owing to the two NH protons. The elemental analyses are in agreement with the structures **14**. Refluxing the latter compound in sodium ethoxide solution gave **15**. The chemical structure of the isolated product **15** was proved from correct analytical and spectral data (see Scheme 4 and experimental).

In the same manner, compounds **5** condensed with azosalicylaldehyde derivatives **16a-d** in *N*,*N*-dimethylformamide (DMF) in the presence of few drops of piperidine afforded in each case, brown solid **18a-d** of melting point above 300 °C (Scheme 5). The structure of the

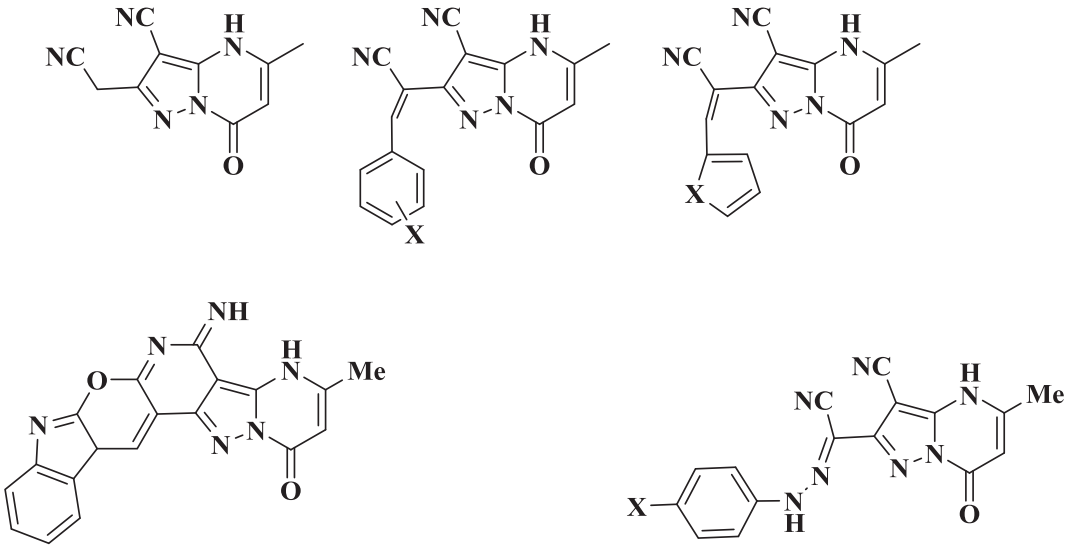

Fig. 4. Our target compounds.

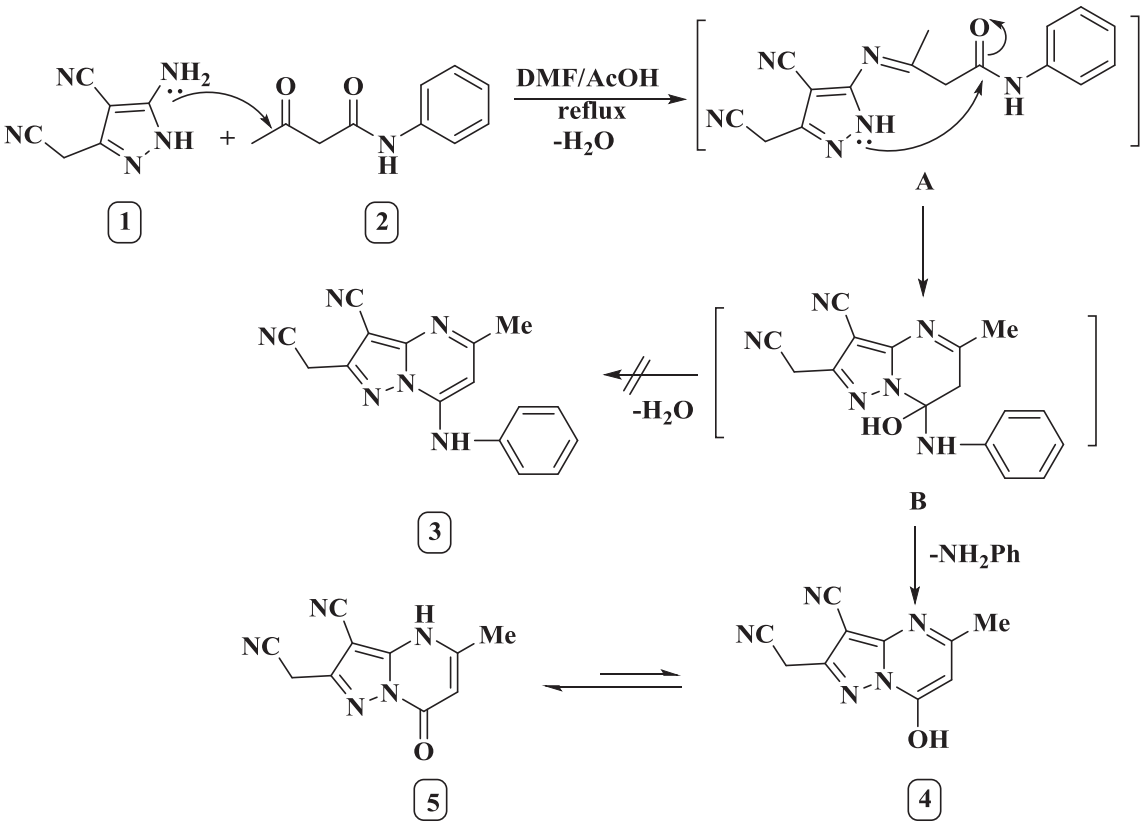

Scheme 1. Synthetic route to 2-(cyanomethyl)-5-methyl-7-oxo-4,7-dihydro-pyrazolo[1,5-*a*]pyrimidine-3-carbonitrile **5**.

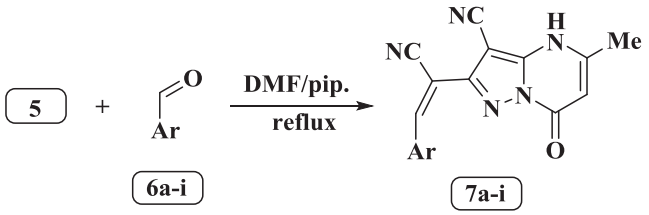

7	Ar	7	Ar
a	Ph	f	2-thienyl
b	4-$OMeC_6H_4$	g	2,5-$(OMe)_2C_6H_3$
c	4-ClC_6H_4	h	3,4,5-$(OMe)_3C_6H_2$
d	3,4$(OCH_2O)C_6H_3$	i	4-OH, 3-$OMeC_6H_3$
e	2-furyl		

Scheme 2. Synthetic route to 2-(1-cyano-2-arylvinyl)-5-methyl-7-oxo-4,7-dihydro-pyrazolo[1,5-*a*]pyrimidine-3-carbonitrile**7a-i.**

isolated products **18a-d** was confirmed by elemental analyses and spectral data (see Scheme 5 and experimental). The latter compounds were converted into azopolyheterocyclic compounds through refluxing in sodium ethoxide solution to give products **19a-d**. The structure of the isolated products **19a-d** was proved from correct analytical and spectral data. As typical example, the IR spectrum of **19c** showed disappearance of an absorption band corresponding to nitrile group near to ν_{max} ~2200 cm^{-1} and instead revealed an absorption band at ν_{max} 3180 cm^{-1} due to NH group. The ^1H NMR spectrum of **19c** revealed a D_2O-exchangeable signal at δ = 9.02 ppm attributable to NH proton.

Finally, we extended our presented study to synthesize new azodye derivatives. Thus, compound **5** was coupled with the diazotized aromatic amines **20a-d** in *N*,*N*-dimethylformamide (DMF) in the presence of sodium hydroxide at 0–5 °C leading to red colored compounds **21a-d** (Scheme 6). The IR spectrum of the isolated compound **21d** taken as a typical example of the prepared series, showed absorption bands at ν_{max} 3424, 2216 and 1635 cm^{-1} corresponding to the 2NH, 2CN and CO groups, respectively. The ^1H NMR spectrum of **21d** revealed a singlet signal at δ = 5.76 ppm due to pyrimidine proton, in addition, a D_2O-exchangeable signal appeared at δ = 12.81 ppm assigned to the NH proton, beside the other expected signals for aryl protons. The mass spectrum of **21d** exhibited a correct molecular ion peak at *m/z* = 353 (M^+ + 2).

The electronic absorption spectra of the products **21a-d** in DMF revealed, in each case, two absorption bands in the regions λ_{max} 447–418 and 305–263 nm. This absorption pattern seems to indicate that the studied compounds **21a-d** exist predominantly in solution as hydrazone form **A**. This is because such an absorption pattern is similar to that of typical hydrazones [31,32]. ^1H NMR spectra provide an additional evidence that they have the hydrazone form **A** rather than the azo-forms **B**. For example, the ^1H NMR spectrum of compounds **15** in DMSO-d_6 exhibit, in each case, one singlet signal near δ 12.0 ppm due to the ═NNH-proton and this is substantiated by the literature data which indicate that the chemical shift (δ) of hydrazone NH resonance is usually observed near 13.0 ppm [33] (see Table 1).

2.2. Biology

2.2.1. Anticancer evaluation

The in *vitro* cytotoxic activity of some newly synthesized pyrazolo [1,5-*a*]-pyrimidine derivatives **5**, **7a**, **7b**, **7c**, **7e**, **7h**, **7i**, **15**, **21a** and **21c,d** was determined by MTT assay (a colorimetric method) against two human cancer cell lines: human breast adenocarcinoma (MCF-7) and human epithelial cervical carcinoma (Hela) (Table 2, Fig. 5) using Doxorubicin as a reference drug.

The results of cytotoxic activity are expressed as concentration IC_{50} (μM/ml). IC_{50} define as the concentration of drug required to inhibit 50% of cell growth.

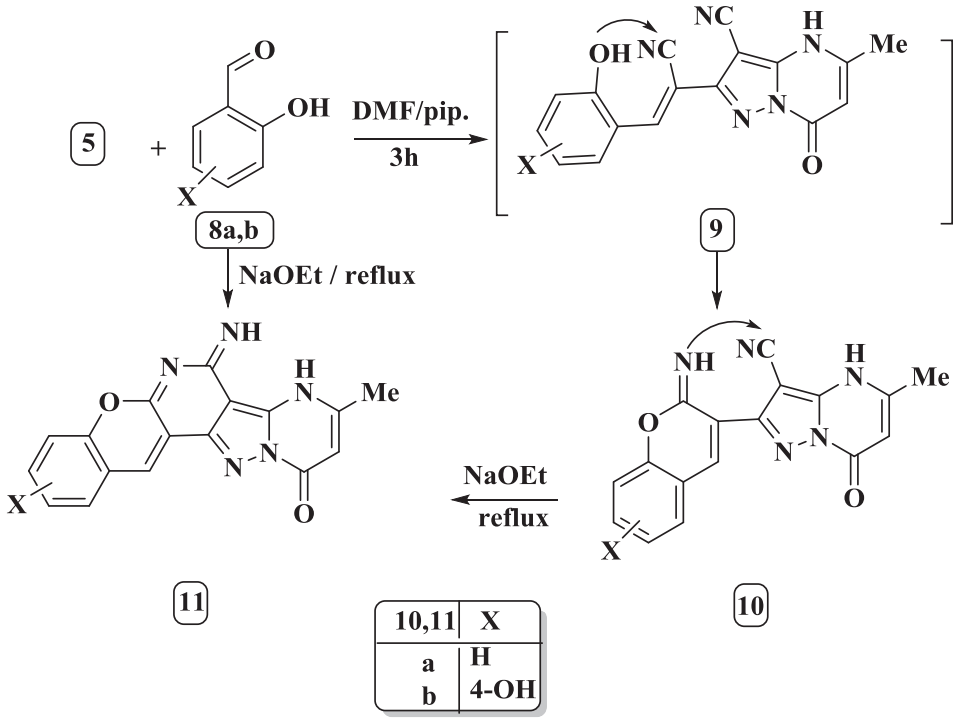

Scheme 3. Synthetic pathway to 2-(2-imino-2*H*-chromen-3-yl)-5-methyl-7-oxo-4,7-dihydropyrazolo[1,5-*a*]pyrimidine-3-carbonitrilederivatives **10a,b** and fused pyrazolo[1,5-*a*]pyrimidine **11a,b.**

According to the previous presented results in (Table 2), it was concluded that the parent compound **5** has strong and moderate cytotoxic activity against both breast and hela cancer cell lines with IC_{50} = 13.91 ± 1.4 and 22.37 ± 1.8 μM/L, respectively. When phenyl group was introduced in the parent compound, the cytotoxic activity decreases with respect to both human cancer cell lines with IC_{50} = 19.70 ± 1.8 and 28.58 ± 2.6 μM/L, respectively. In case of introducing substituted phenyl group to parent compound **5** the cytotoxic activity highly decreased in case of electron donating and electron withdrawing such as 4-methoxyphenyl and 4-cholorophenyl groups but still electron donating has higher cytotoxic activity than electron withdrawing with respect to both human cancer cell lines (for 4-methoxy: IC_{50} = 64.14 ± 3.6 and 71.62 ± 4.3 μM/L) and (for 4-chloro: IC_{50} = 74.26 ± 4.2 and 88.16 ± 5.1 μM/L), respectively. On the other hand, when introduced phenyl group bearing more than one electron donating groups such as trimethoxyphenyl which carry the same electron donating species the cytotoxic activity (IC_{50} = 34.22 ± 2.7 and 45.01 ± 3.5 μM/L) improved than monomethoxyphenyl group with breast and hela cell lines, respectively. But when the electron donating groups introduced are different species as

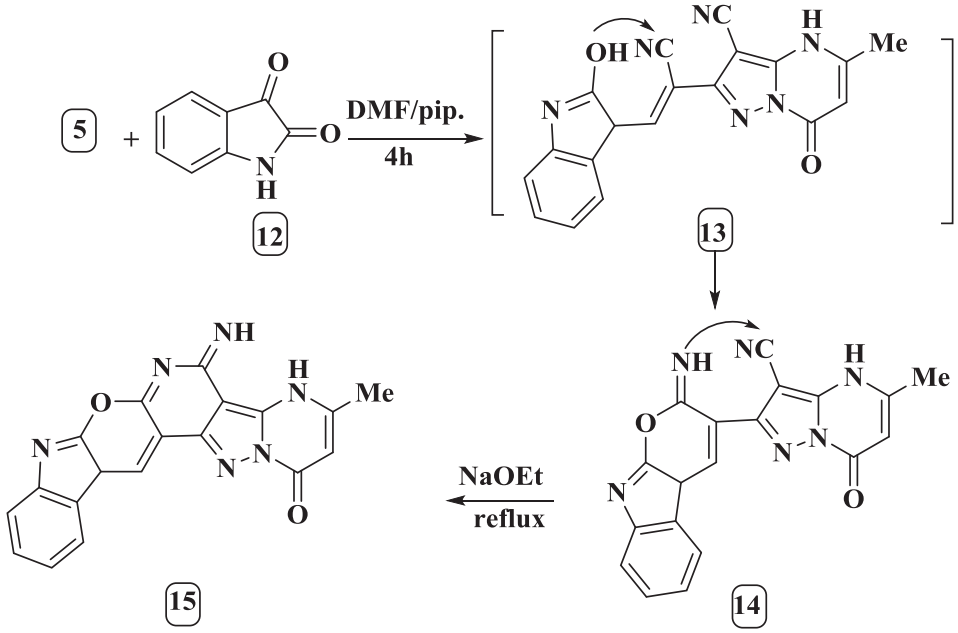

Scheme 4. Synthetic pathway to pyrano[2,3-*b*]indol-3-yl)-5-methyl-7-oxo-4,7-dihydropyrazolo[1,5-*a*]pyrimidine-3-carbonitrile **14** and fused pyrazolo[1,5-*a*]-pyrimidine **15.**

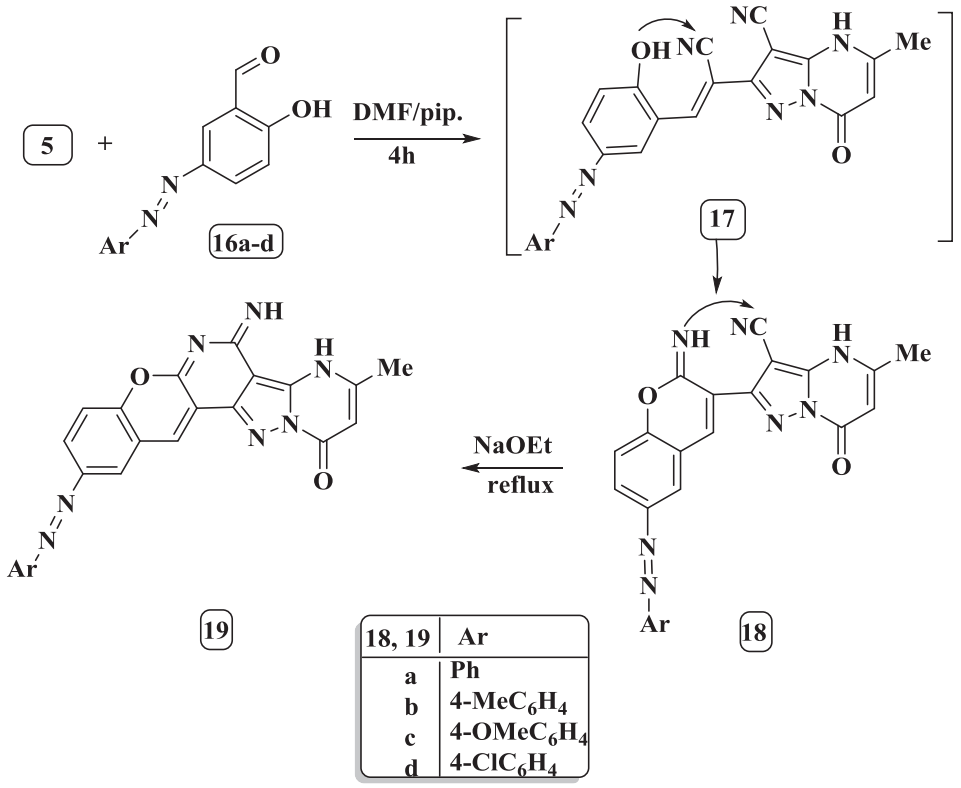

Scheme 5. Synthetic pathway to 2-(2-imino-6-(aryldiazenyl)-2*H*-chromen-3-yl)-5-methyl-7-oxo-4,7-dihydropyrazolo[1,5-*a*]pyrimidine-3-carbonitrile derivatives **18a-d** and fused pyrazolo[1,5-*a*]pyrimidine **19a-d.**

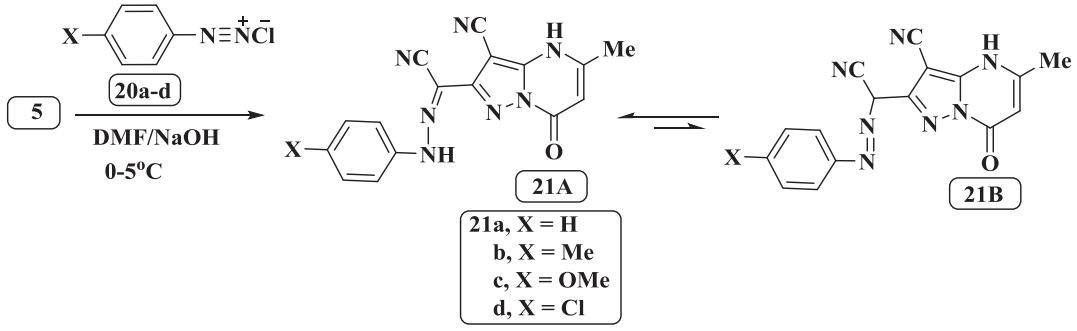

Scheme 6. Synthetic pathway to 3-cyano-5-methyl-7-oxo-*N*-phenyl-4,7-dihydro-pyrazolo[1,5-*a*]pyrimidine-2-carbohydrazonoyl cyanide derivatives **21a-d.**

Table 1
Electronic absorption spectral data of compounds **21a-d** in *N,N*-dimethylformamide (DMF).

Compound no.	λ_{max}(nm) DMF
21a	390–303
21b	445–305
21c	304–261
21d	447–263

hydroxyl and methoxy groups, the cytotoxic activity become very strong with both breast and hela with IC_{50} = 9.48 ± 0.8 and 10.63 ± 1.0 μM/L, respectively near standard drug Doxorubicin.

In contrast to phenyl and substituted phenyl group, introducing hetero- moiety like furan to the parent compound which gave the highest cytotoxic activity among the all tested compounds against both breast and hela cancer cell lines with IC_{50} = 6.56 ± 0.5 and 8.72 ± 0.9 μM/L, respectively and this result close to Doxorubicin with IC_{50} = 4.17 ± 0.2 and 5.57 ± 0.4 μM/L.

Table 2
IC_{50} of the tested compounds against two human cell lines using Doxorubicin as a reference drug.

Tested compounds	Human cancer cell lines	
	MCF-7 IC_{50} (μM/ml)	HeLa IC_{50} (μM/ml)
5	13.91 ± 1.4	22.37 ± 1.8
7a	19.70 ± 1.8	28.58 ± 2.6
7b	64.14 ± 3.6	71.62 ± 4.3
7c	74.26 ± 4.2	88.16 ± 5.1
7e	6.56 ± 0.5	8.72 ± 0.9
7h	34.22 ± 2.7	45.01 ± 3.5
7i	9.48 ± 0.8	10.63 ± 1.0
15	26.08 ± 2.2	37.49 ± 3.1
21a	56.28 ± 3.5	32.74 ± 2.8
21c	64.87 ± 3.7	41.16 ± 3.4
21d	68.14 ± 4.0	60.93 ± 4.3
Doxorubicin	4.17 ± 0.2	5.57 ± 0.4

IC_{50} (μM/ml) are expressed as mean ± SD.

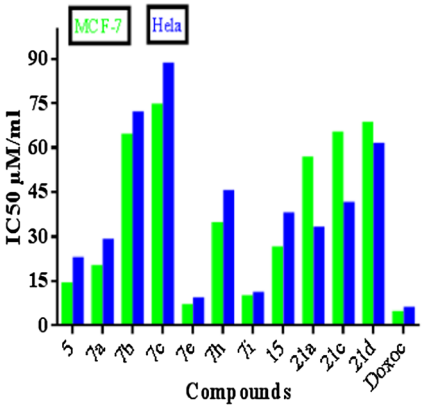

Fig. 5. Cytotoxic activity of the target compounds (**5**, **7a-c**, **7e**, **7h**, **7i**, **15**, **21a**, **21c** and **21d**) against the tumor MCF-7 and hela cell lines.

Depending on the above data and the structure-activity relationship (SAR) for the tested compounds against breast and hela cancer cell lines indicated that the pyrazolo[1,5-*a*]pyrimidine derivatives that bearing hetero- moiety have the highest cytotoxic activity as compound **7e** with IC_{50} = 6.56 ± 0.5 and 8.72 ± 0.9 µM/L than those bearing phenyl and substituted phenyl group. In spite of, substituted phenyl group with electron withdrawing group such as 4-choloro phenyl gave the lowest cytotoxic activity with IC_{50} = 74.26 ± 4.2 and 88.16 ± 5.1 µM/L of all tested compounds against two human cancer cell lines (breast and hela).

2.2.2. KDM inhibitory assay

KDM inhibition activity was investigated by ELISA assay for the most potent cytotoxic active compounds **5**, **7e** and **7i** using MCF-7 cancer cell, the results deduced from Table 3 showing that all tested compounds **5**, **7e** and **7i** exhibited potent inhibitory effect toward KDM with IC_{50} = 4.05, IC_{50} = 1.91 and IC_{50} = 2.31 µM, respectively. This mean that the tested compounds may induce their inhibitory effect by binding to KDM enzyme active site and inhibition of its activity cause cancer cell death.

2.2.3. In vitro DNA-flow cytometric (cell cycle) analysis

Also, the present work extending by electing the more potent inhibitory active compound **7e** and investigate its effect on cell cycle progression and apoptosis induction in MCF-7 cell line. Cell cycle phases were determined by flow cytometry after propidium iodide (PI) staining. The MCF-7 cells were incubated with 10 µM of compound **7e** for 48 h, and then its effect on cell cycle phases was analyzed, DMSO used as a negative control. The results obtained from exposure of MCF-7 cell to compound **7e** refer that this compound cause a significant increase in the percentage of cells at phases of preG1 (which could be indicative of apoptosis) and G2/M (DNA repair and mitosis) by 10 and 4 folds respectively, compared to control. These results indicated that compound **7e** arrest MCF-7 cancer cells at G2/M phase of cell cycle (Table 4 and Figs. 6 and 7).

2.2.4. Annexin V-FITC apoptosis assay

Annexin V binding study was performed to determine early and late apoptosis employing flow cytometer where Annexin V conjugated with FITC is used to stain cells in combination with propidium iodide (PI). The cells in the late apoptotic stage that have loss membrane integrity [34] are represented as a stained positive for Annexin V/PI. The apoptotic value of compound **7e** on MCF-7 cells was determined *via* flow cytometry detection using Annexin V/propidium iodide (PI) double staining assay when MCF-7 cells treated with 10 µM of compound **7e** for 48 h. The results was obtained indicated that early apoptosis ratio (lower right quadrant of the cytogram) increases by about 13 fold and the late apoptosis ratio (higher right quadrant of the cytogram) increases by about 34 fold, and this mean that compound **7e** proved to induce apoptosis by 13.94% (Table 5 and Fig. 8).

Table 3
Inhibitory activity in *vitro* for compounds **5**, **7e** and **7i** against KDM.

Compound number	KDM IC_{50} (µM)
5	4.05 ± 0.29
7e	1.91 ± 0.12
7i	2.31 ± 0.17

2.2.5. In silico studies of anticancer activity

Lipiniski's rule of five (the effect of lipophilic and steric parameters)

Computational studies were carried out for the more potent cytotoxic compounds; lipiniski's parameters and topological polar surface area (TPSA) were predicted from Swiss ADME (absorption, distribution, metabolism and excretion). Lipinski's rule states that for molecules to be taken orally should satisfied these rules: (i) Not more than 5 hydrogen donors (ii) Not more than 10 hydrogen acceptors (iii) Molecular weight < 500 (iv) calculated logP < 5. To be considered as an orally active drug it should has no more than one violation, if more than one violation it might have problems in bioavailability [35]. As shown in Table 6, compound **5**, **7e** and **7i** are in agreement with the parameters of lipinisk's rule and this indicate that these compounds have promising drug like properties. Topological polar surface area (TPSA) is defined as the surface sum over all polar atoms or molecules, usually oxygen and nitrogen, including their attached hydrogen atoms. Polar surface area (PSA) used for optimization of drug's ability to permeate cell, thus molecule with PSA greater than 140$Å^2$ have poor ability to permeate cell membranes [36]. The new prepared compounds **5**, **7e** and **7i** have TPSA equals 97.74, 110.88 and 127.20 $Å^2$, respectively. These values mean that the target compounds **5**, **7e** and **7i** can permeate cell membranes (Table 6).

2.2.6. Molecular modeling and docking study

Molecular docking study was performed to gain insight in to the most preferred binding mode of compound into the enzyme binding active site. The binding affinity of the ligand with the active site of enzyme was determined by energy score (S, Kcal/mol), low energy score indicates good affinity. Hydrogen bond, arene-arene and arene-cation interaction are the mode of interaction presented in molecular docking. The target-ligand interaction determined by molecular docking of both protein as a target and some tested compounds as a ligand. Molecular docking was performed through using crystal structure of KDM5A protein that deduced from protein data bank (PDB- ID: 5IVE) and the most stable conformation of some tested compounds. Target-ligand stimulation for some newly synthesized compounds **5**, **7c**, **7e** and **7i** was carried out using the Molecular Operating Environment (MOE 2009.10) software (see Table 7).

Self docking of the native ligand with the active site of the selected protein showed two arene-arene interactions along with two for hydrogen bonds. The first hydrogen bond formed between oxygen linked to C_4 of ring A and NH_2 of Lys501(1.93 Å), and the second between CN linked to C_9 of ring B and nitrogen (N) of His483 (3.18 Å) with binding energy (S = −10.6852) Kcal/mol (Fig. 9). The mode of interactions for compounds **7e** and **7i** which appeared the highest potency against KDM5A with both human cancer cell lines (breast and hela) was illustrated. Thus compound **7e** showed five interactions three of them for arene-arene interactions and rest two for hydrogen bond. One of the hydrogen bond is between CN linked to C_9 of ring B (pyrazole ring) and OH of Tyr 472(2.31Å), the other hydrogen bond is between CN linked to C_{10} attached to C_8 of ring B (pyrazole ring) and OH of Tyr

Table 4
Results of cell cycle analysis in MCF-7 expressed by (%) of cell in each phase when treated with compound **7e**.

Compound number	%G0-G1	%S	%G2-M	%Pre-G1	Comment
7e/MCF7	30.93	14.16	54.91	19.22	PreG1apoptosis&Cell growth arrest at G2/M
MCF7	55.21	29.81	14.98	2.02	

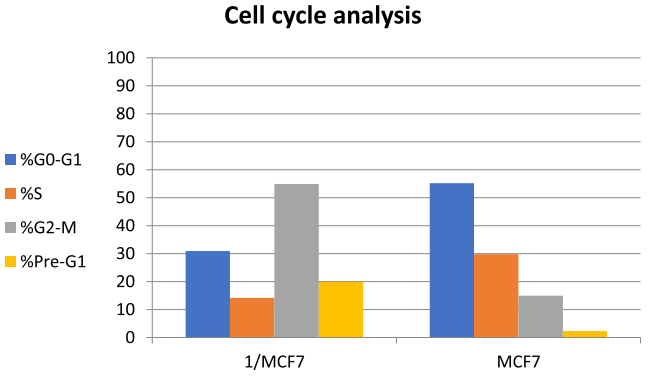

Fig. 6. Cell cycle and apoptosis effect in MCF-7 cell line treated with compound **7e**.

Table 5
Results of cell cycle analysis in MCF-7 expressed by (%) of cells in each phase when treated with compound **7e**.

Compound number	Apoptosis %			Necrosis
	Total	Early	Late	
7e/MCF7	19.22	4.56	9.38	5.28
Cont. MCF7	2.02	0.36	0.28	1.38

409(3.68 Å) with binding energy (S = −10.8091) Kcal/mol (Fig. 10). Also, compound **7i** exhibited four interactions one of them for arene-arene interaction and the other three for hydrogen bonds. The first hydrogen bond is between oxygen linked to C_4 of ring A and NH_2 of Arg73(2.16 Å), and the other two hydrogen bonds between OCH_3 linked to ring C and Asn 575 (1.56 Å), Lys 501 (2.29 Å) with binding energy (S = −12.2875) Kcal/mol (Fig. 11). Moreover, the molecular docking of the parent compound **5** with active site of enzyme; presented

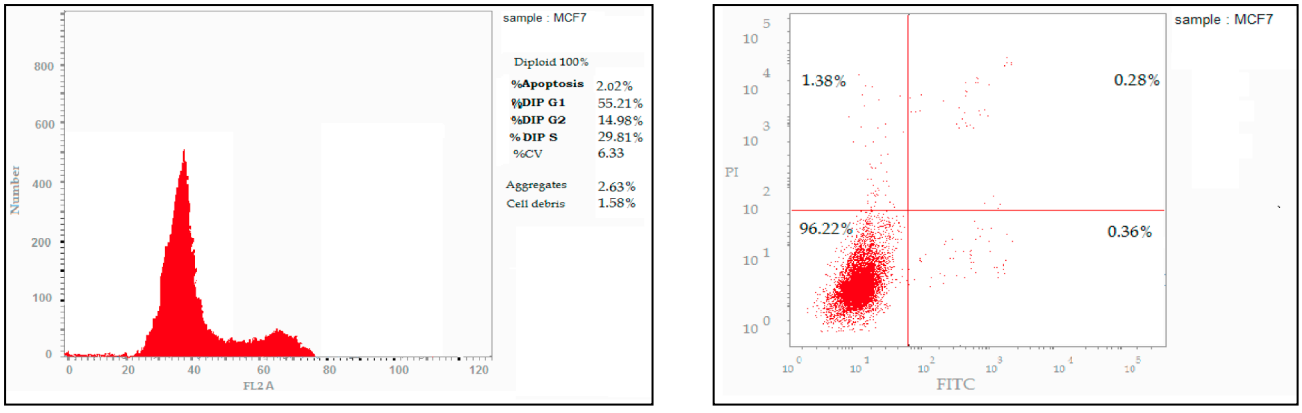

I. Control MCF-7

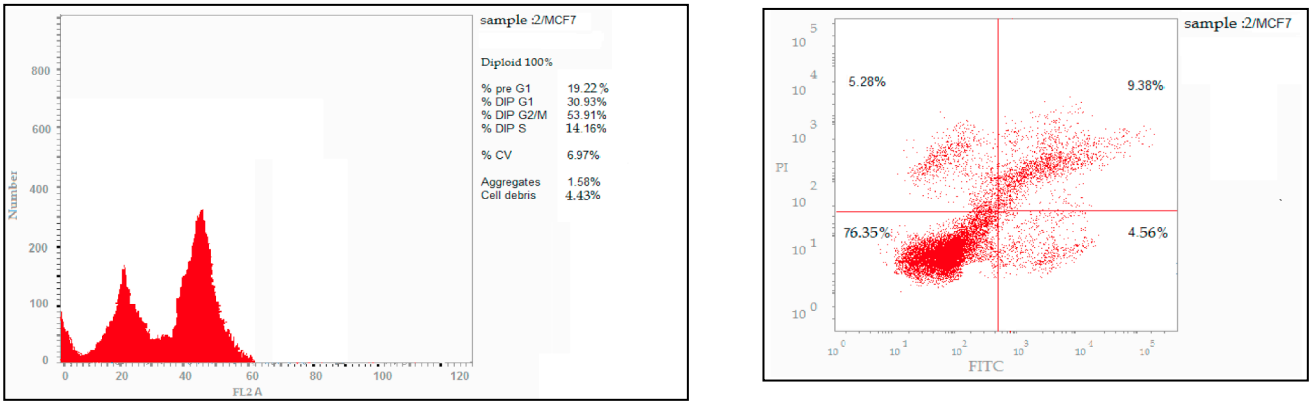

II. 7e/ MCF-7

Fig. 7. Cell cycle: I. control MCF-7, II. Compound **7e** by flow cytometery using PI staining method.

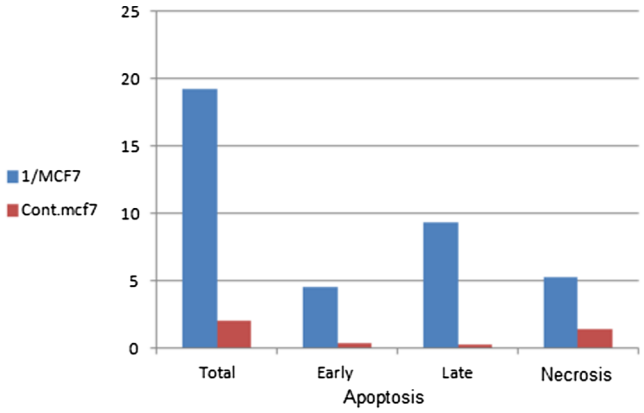

Fig. 8. Percent of cell death induced by compound **7e** on MCF-7 cells.

Table 6
Lipiniski's parameters and TPSA of the more potent cytotoxic compounds.

Comp. no.	TPSA (Å^2)	Lipinisk's parameters				
		Log P	M. W.	nHBD (OHNH)	nHBA (NO)	No. of viol
5	97.74	0.52	213.20	1	4	0
7e	110.88	1.48	291.26	1	5	0
7i	127.20	1.76	347.33	2	6	0

nHBD = number of hydrogen bond donor.
nHBA = number of hydrogen bond acceptor.

three interactions two of them for arene-arene interactions and last for hydrogen bond between CN linked to C_9 of ring B (pyrazole ring) and NH_2 of Asn 493 (2.77 Å) with binding energy (S = −9.1748) Kcal/mol (Fig. 12). Molecular docking of compound **7c** which has the lowest cytotoxic activity showed only one interaction for hydrogen bond between CN linked to C_9 of ring B (pyrazole ring) and NH_2 of His 483(2.96 Å) with binding energy (S = −8.2989) Kcal/mol (Fig. 13).

2.2.7. Bioinformatics studies

Drug discovery was supported by study physicochemical descriptors, ADME parameters, pharmacokinetic properties, drug like nature and medicinal chemistry for one or multiple small molecules. The molecule is first described by its 2D chemical structure and canonical SMILES together with the bioavailability radar to estimate oral bioavailability at first glance (see Fig. 14).

The various models and data are grouped in different sections of the one-panel-per-molecule output (physicochemical properties, lipophilicity, pharmacokinetics, drug likeness and medicinal chemistry). Apart from efficacy and toxicity, many drug development failures are imputable to poor pharmacokinetics and bioavailability. Gastrointestinal absorption and brain access are two pharmacokinetic behaviors crucial to estimate at various stages of the drug discovery processes.

Bioinformatics studies for compounds **7e** and **7i** are performed on Swiss ADME (Swiss Institute of bioinformatics 2018).

Absorption, distribution, metabolism and excretion (ADME), Topological polar surface area (TPSA), gastrointestinal absorption (GI absorption), blood brain barrier (BBB) permeant, P-glycoprotein substrate (P-gp substrate), pan-assay interference structure (PAINS).

Firstly, TPSA (topological polar surface area) defined as the surface sum of all polar atom, primarily oxygen and nitrogen also including their attached hydrogen atom. PSA used for optimization of drug's ability to permeate cell, molecule with PSA greater than 140 Å^2 have poor permeating cell membranes [36]. Thus, from data depicted in Table 8 showed physicochemical properties of compounds **7e** and **7i** which appeared that compounds **7e** and **7i** have TPSA 110.88 and 127.20 Å^2, respectively. These values mean that the compounds **7e** and

Table 7
Protein-ligand interactions of some tested compounds with KDM5A active site pocket.

Compound number	Binding energy (S) (Kcal/mol)	Groups of the ligand involved in the interaction	Amino acids involved in the interaction	Type of the Bond and length of Hydrogen bonds (Å)
7e	−10.8091	Cyano (CN)	Tyr 472	Polar sidechain acceptor 2.13 Å
		Cyano (CN)	Tyr 409	Polar sidechain acceptor 3.68 Å
		Pyrazole ring	His 483	Basic backbone acceptor (Arene-Arene interaction)
		Furan ring	Tyr 472	Polar sidechain acceptor (Arene-Arene interaction)
		Furan ring	Phe 480	Greasy backbone donor (Arene-Arene interaction)
7i	−9.6461	Carbonyl (CO)	Arg 73	Basic backbone acceptor 2.16 Å
		Methoxy (OCH_3)	Lys 501	Basic backbone acceptor 2.29 Å
		Methoxy (OCH_3)	Asn 575	Polar sidechain acceptor 1.56 Å
		Phenyl ring	Tyr 409	Polar sidechain acceptor (Arene-Arene interaction)
5	−9.1748	Cyano (CN)	Asn493	Polar sidechain acceptor 2.77 Å
		Pyrazole ring	Tyr 472	Polar sidechain acceptor (Arene-Arene interaction)
		Pyrazole ring	Phe 480	Greasy backbone donor (Arene-Arene interaction)
7c	−8.2989	Cyano (CN)	His 483	Basic backbone acceptor 2.96 Å
Validation	−10.6852	Cyano (CN)	His 483	Basic backbone acceptor 3.18 Å
		Cyano (CN)	Lys 501	Basic backbone acceptor 1.93 Å
		Pyrazole ring	Tyr 472	Polar sidechain acceptor (Arene-Arene interaction)
		Pyrazole ring	Phe 480	Greasy backbone donor (Arene-Arene interaction)

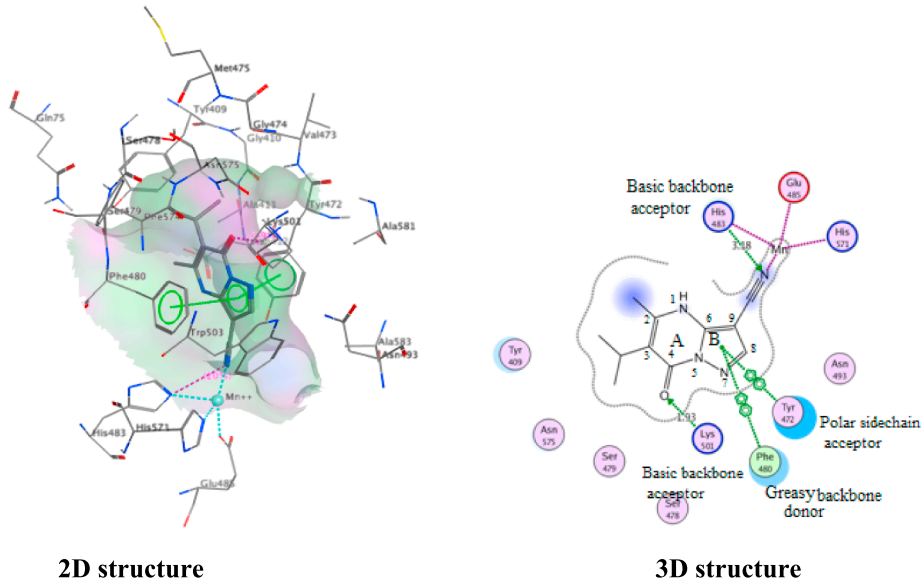

Fig. 9. Binding pattern of the native ligand (2D and 3D) structure with its active site of the protein KDM5A (PDB: 5IVE).

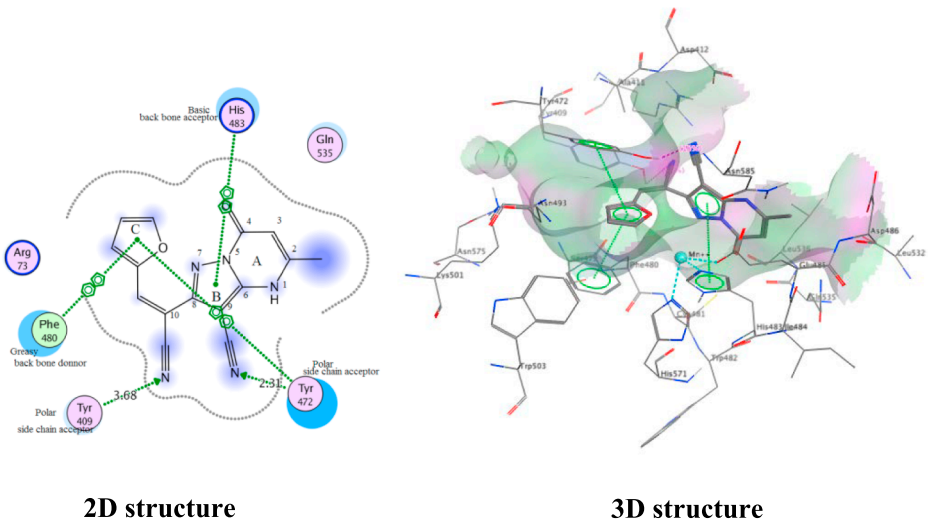

Fig. 10. Binding pattern of compound **7e** (2D and 3D) structure with the active site of the selected protein KDM5A (PDB: 5IVE).

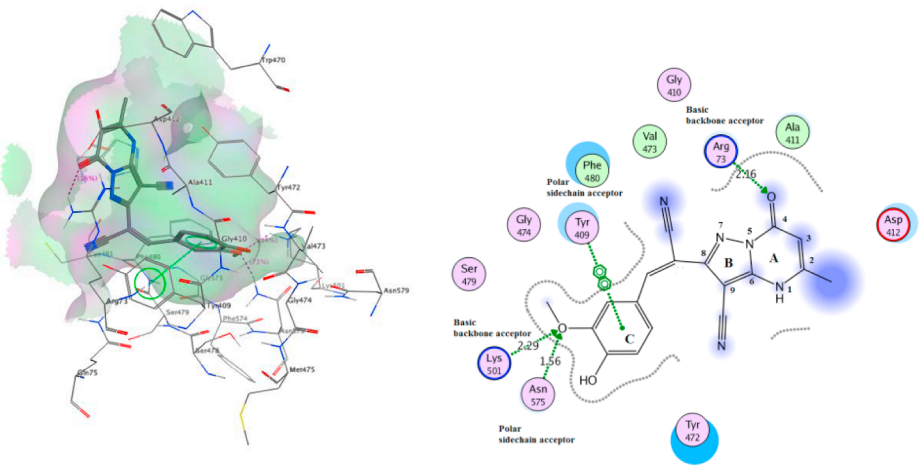

Fig. 11. Binding pattern of compound **7i** (2D and 3D) structure with the active site of the selected protein KDM5A (PDB: 5IVE).

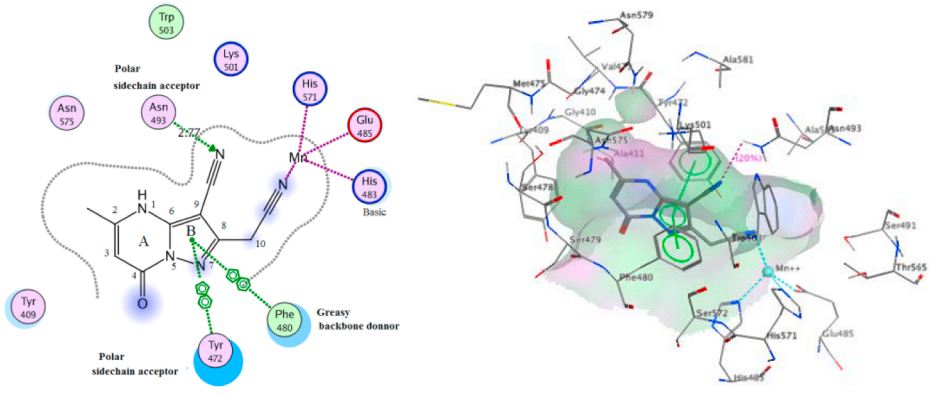

Fig. 12. Binding pattern of compound **5** (2D and 3D) structure with the active site of the selected protein KDM5A (PDB: 5IVE).

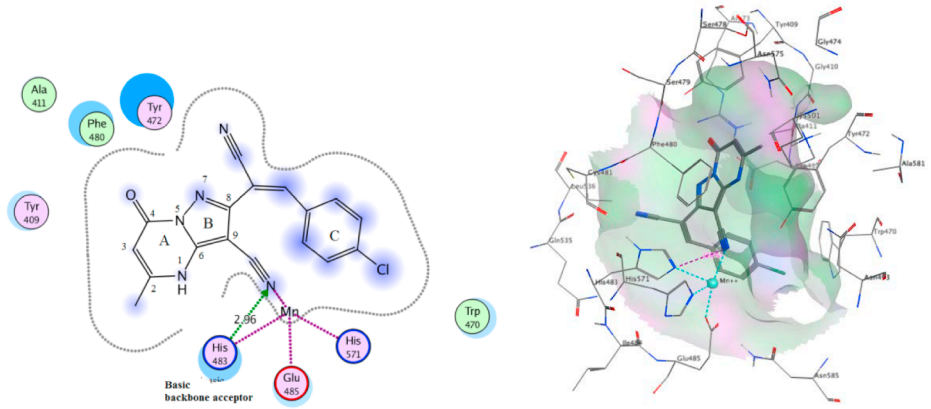

Fig. 13. Binding pattern of compound **7c** (2D and 3D) structure with the active site of the selected protein KDM5A (PDB: 5IVE).

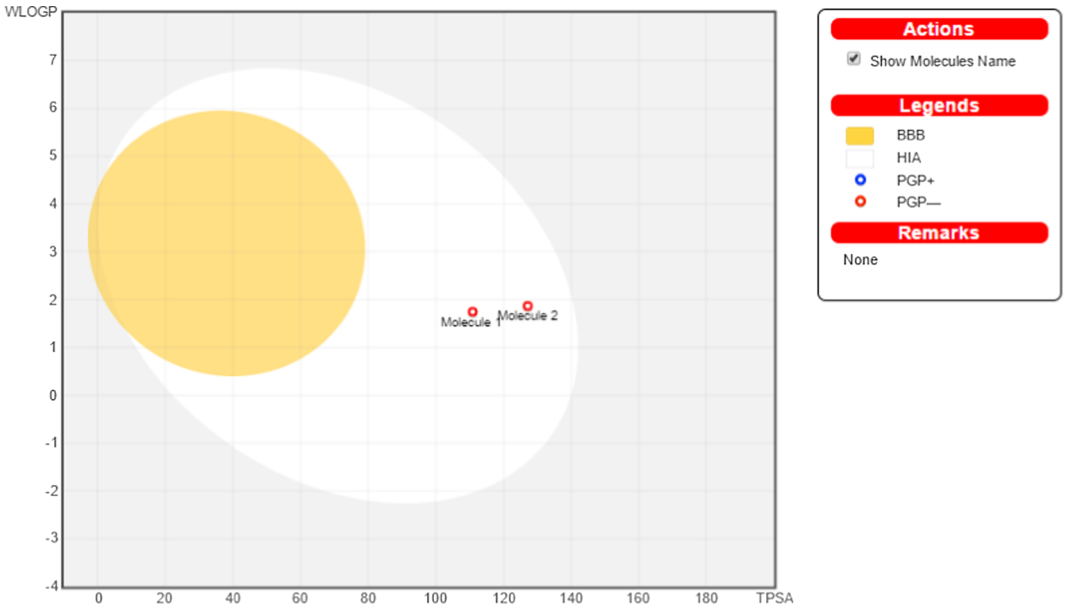

Fig. 14. (BOILED-Egg) model of compounds **7e** (molecule 1) and **7i** (molecule 2).

Table 8
Bioactivity and ADME toxicity according to Lipinski's rule five.

Compounds	7e	7i
Molecular weight	291.26 g/mol	347.33 g/mol
Num. rotatable bonds	2	3
Num. H-bond acceptors	5	6
Num. H-bond donors	1	2
Molar refractometry	77.69	93.93
TPSA	110.88 Å^2	127.20 Å^2
Consensus Log Po/w	1.48	1.76
GI absorption	High	High
BBB permeant	No	No
P-gy substrate	No	No
Cytochrome P450	CYP1A2 inhibitor	CYP2C9 inhibitor
Log Kp (skin permeation)	−7.14 cm/s	−7.12 cm/s
Lipinski	Yes; 0 violation	Yes; 0 violation
Bioavailability score	0.55	0.55
PAINS	0 alert	0 alert
Leadlikeness	Yes	Yes
Synthetic accessibility	3.06	3.17

7i can permeate cell membranes. Consensus lipophilicity of compounds **7e** and **7i** is 1.48 and 1.76, respectively, that showed low lipophilicity so that these compounds cannot permeate BBB (blood brain barrier).

Pharmacokinetics studies are important in drug discovery process, gastrointestinal absorption and brain access are two pharmacokinetics behavior, thus the two studied compounds **7e** and **7i** are highly absorbed in gastrointestinal but can't pass BBB or be P-glycoprotein substrate. From this collective data, it can deduced the method of administration include oral and sublingual (dissolving the drug under the tongue). In addition, in pharmacokinetics, the permeability can be estimated *via* skin by permeability coefficient (Kp), the permeability coefficient of compounds **7e** and **7i** is −7.14 and −7.12 Cm/s, respectively. Additionally, medicinal chemistry showed that synthetic accessibility with 3.06 and 3.17 for compounds **7e** and **7i**, respectively. These values mean that two compounds easily synthesized.

2.2.8. BOILED-Egg (Brain or IntestinaL EstimateD penetration) model

(BOILED-Egg) is proposed as an accurate predictive model that worked by computing the lipophilicity and polarity of small molecule.

- White ellipse represents compounds with high probability to be passively absorbed by the gastrointestinal tract.
- Yellow ellipse represents compounds with high probability to permeate through BBB to access CNS.
- Grey zone represents molecules that not predicted to be well absorbed nor BBB permeate.
- Blue point: molecule predicted to be substrate of the p-glycoprotein (PGP+).
- Red point: molecule predicted to be non substrate of the p-glycoprotein (PGP−).

The (BOILED-Egg) model of compounds **7e** (molecule 1) and **7i** (molecule 2) showed that the two compounds appear in the white ellipse that mean compounds absorbed by the gastrointestinal tract and appear as red point that mean compounds not substrate to P-glycoprotein.

3. Conclusion

Some novel pyrazolo[1,5-*a*]pyrimidine derivatives were synthesized and evaluated in *vitro* against breast and hela cancer cell lines. Furthermore, the most potent KDM inhibitor **7e** (IC_{50} = 1.91 μM) showed to cause cell cycle arrest at G2/M phase by 4 folds than control and induce total apoptotic effect by 10 folds more than control.

4. Experimental

4.1. Chemistry

4.1.1. General

Melting points were determined on an Electrothermal (9100) apparatus and are incorrect. The IR spectra were recorded as KBr pellets on a Perkin Elmer 1430 spectrophotometer. ^{1}H NMR and ^{13}C NMR spectra were recorded in deuterated dimethylsulfoxide at 300 and 75 MHz, respectively, on a Varian Gemini NMR spectrometer using tetramethylsilane as internal reference and the results are expected as δ value. Mass spectra were taken on a Shimadzu GCMS-QP 1000 Ex mass spectrometer at 70 eV. UV spectra and elemental analyses were carried out at the Microanalyses Center of Cairo University, Giza, Egypt.

4.1.2. 5-Amino-3-cyanomethyl-1H-pyrazole-4-carbonitrile *1*

To a solution of (2.64 g, 0.02 mol) of 2-aminoprop-1-ene-1,1,3-tricabonitrile in 20 ml of boiling ethanol was added (1.1 g, 0.022 mol) 85% hydrazine hydrate at such a rate that the reaction mixture continued to boil without external heating. The strongly exothermic reaction was accompanied by a vigorous evolution of ammonia. After addition of the hydrazine hydrate was completed, the reaction mixture was allowed to cool slowly to room temperature. The solid so formed was filtered off and recrystallized from glacial acetic acid to give compound **1**. Yield: (74%), mp. = 198 °C [lit. 197–199 °C][37], ν_{max}/cm^{-1} (KBr) 2261 (CN), 2218 (CN); ^{1}H NMR (DMSO) δ = 4.36 (2H, s, CH_2); 6.38 (2H, s, NH_2); 11.41 (1H, s, NH). Anal. Calcd for $C_6H_5N_5$: C, 48.98; H, 3.43; N, 47.60. Found: C, 48.79; H, 3.61; N, 47.84%.

4.1.3. 2-(Cyanomethyl)-5-methyl-7-oxo-4,7-dihydropyrazolo[1,5-a] pyrimidine-3-carbonitrile *5*

A mixture of 5-amino-2-cyanomethyl-1*H*-pyrazole-4-carbonitrile **1** (0.01 mol) and acetoacetanilide **2** (0.01 mol) in *N,N*-dimethylformamide (20 ml) in the presence of few drops of glacial acetic acid was refluxed for 6 h, then poured on cold water. The solid was collected by filtration and recrystallized from *N,N*-dimethylformamide. Brown crystals, yield 53%, m.p > 300 °C, ν_{max}/cm^{-1} (KBr) 3152 (NH), 2227 (2CN), 1671 (CO); ^{1}H NMR (DMSO) δ = 2.38 (s, 3H, CH_3), 4.36 (s, 2H, CH_2), 5.87 (s, 1H, pyrimidine-H), 13.35 (s, 1H, NH); *m/z* = 213 (M^+, 100%), 184 (17.4%), 172 (15.7%), 156 (11.9%), 145 (12.7%), 77 (16.6%), 67 (99.2%); Anal. Calcd for $C_{10}H_7N_5O$: C, 56.34; H, 3.31; N, 32.85. Found: C, 56.51; H, 3.49; N, 32.66%.

4.1.4. General procedure for preparation of compounds *7a-i*

A solution of compound **5** (0.01 mol) in *N,N*-dimethylformamide (10 ml) containing few drops of piperidine was added to the appropriate aldehyde **6a-i** (0.01 mol). The mixture was heated under reflux for 4 h and the solid product that precipitated by cooling was filtered off and recrystallized from *N,N*-dimethylformamide to give the respective products **7a-i**. The physical constants and spectral data are shown below:

4.1.4.1. 2-(1-Cyano-2-phenylvinyl)-5-methyl-7-oxo-4,7-dihydropyrazolo [1,5-a]-pyrimidine-3-carbonitrile ***7a***. Yellow crystals, yield 65%, m.p = 280 °C, ν_{max}/cm^{-1} (KBr) 3146 (NH), 2218 (2CN), 1628 (CO); ^{1}H NMR (DMSO) δ = 2.20 (s, 3H, CH_3), 5.56 (s, 1H, pyrimidine-H), 7.56–7.96(m, 5H, Ar), 8.14 (s, 1H, CH), 13.21 (s, 1H, NH); Anal. Calcd for $C_{17}H_{11}N_5O$: C, 67.77; H, 3.68; N, 23.24. Found: C, 67.94; H, 3.52; N, 23.44%.

4.1.4.2. 2-(1-Cyano-2-(4-methoxyphenyl)vinyl)-5-methyl-7-oxo-4,7-dihydropyrazolo-[1,5-a]pyrimidine-3-carbonitrile ***7b***. Brown crystals, yield 74%, m.p > 300 °C, ν_{max}/cm^{-1} (KBr) 3190 (NH), 2222 (2CN), 1650 (CO); ^{1}H NMR (DMSO) δ = 2.50 (s, 3H, CH_3), 3.86 (s, 3H, OCH_3), 5.81 (s, 1H, pyrimidine-H), 7.85 (d, 2H, *J* = 8.4 Hz, Ar), 7.94 (d, 2H, *J* = 8.4 Hz, Ar), 8.06 (s,1H, CH), 9.95 (s, 1H, NH); Anal. Calcd for

$C_{18}H_{13}N_5O_2$: C, 65.25; H, 3.95; N, 21.14. Found: C, 65.42; H, 3.77; N, 21.38%.

4.1.4.3. 2-(2-(4-Chlorophenyl)-1-cyanovinyl)-5-methyl-7-oxo-4,7-dihydropyrazolo-[1,5-a]pyrimidine-3-carbonitrile ***7c***. Brown crystals, yield 66%, m.p > 300 °C, ν_{max}/cm^{-1} (KBr) 3406 (br., NH), 2216 (2CN), 1635 (CO); ^{1}H NMR (DMSO) δ = 2.49 (s, 3H, CH_3), 5.74 (s, 1H, pyrimidine-H), 7.59 (d, 2H, J = 8.7 Hz, Ar), 7.92 (d, 2H, J = 7.5 Hz, Ar), 7.63 (s,1H, CH), 10.31 (s, 1H, NH); m/z = 335 (M^+, 0.3%), 317 (0.9%), 305 (2.5%), 213 (1.4%), 189 (5.8%), 143 (5.2%), 113 (35.0%), 101 (22.8%), 87 (30.5%), 59 (100%); Anal. Calcd for $C_{17}H_{10}ClN_5O$: C, 60.82; H, 3.00; Cl, 10.56; N, 20.86. Found: C, 60.67; H, 3.15; N, 20.64%.

4.1.4.4. 2-(2-(Benzo[d][1,3]dioxol-4-yl)-1-cyanovinyl)-5-methyl-7-oxo-4,7-dihydro-pyrazolo[1,5-a]pyrimidine-3-carbonitrile ***7d***. Brown crystals, yield 70%, m.p > 300 °C, ν_{max}/cm^{-1} (KBr) 3152 (NH), 2215 (2CN), 1671 (CO); ^{1}H NMR (DMSO) δ = 2.29 (s, 3H, CH_3), 5.77 (s, 1H, pyrimidine-H), 6.16 (s, 2H, CH_2), 7.11–8.03 (m, 3H, Ar), 8.26 (s,1H, CH), 9.97 (s, 1H, NH); Anal. Calcd for $C_{18}H_{11}N_5O_3$: C, 62.61; H, 3.21; N, 20.28. Found: C, 62.78; H, 3.06; N, 20.56%.

4.1.4.5. 2-(1-Cyano-2-(furan-2-yl)vinyl)-5-methyl-7-oxo-4,7-dihydropyrazolo[1,5-a]-pyrimidine-3-carbonitrile ***7e***. Brown crystals, yield 84%, m.p > 300 °C, ν_{max}/cm^{-1} (KBr) 3140 (br., NH), 2214 (2CN), 1628 (CO); ^{1}H NMR (DMSO) δ = 2.50 (s, 3H, CH_3), 5.82 (s, 1H, pyrimidine-H), 6.81–7.95 (m, 3H, Ar), 8.09 (s, 1H, CH), 10.62 (s, 1H, NH); m/z = 291 (M^+, 1.3%), 279 (2.9%), 239 (1.8%), 211 (1.5%), 183 (2.3%), 149 (53.2%), 85 (55.6%), 71 (82.0%), 69 (47.1%), 57 (100%); Anal. Calcd for $C_{15}H_9N_5O_2$: C, 61.85; H, 3.11; N, 24.04. Found: C, 61.71; H, 3.28; N, 24.26%.

4.1.4.6. 2-(1-Cyano-2-(thiophen-2-yl)vinyl)-5-methyl-7-oxo-4,7-dihydropyrazolo[1,5-a]-pyrimidine-3-carbonitrile ***7f***. Brown crystals, yield 91%, m.p > 300 °C, ν_{max}/cm^{-1} (KBr) 3422 (br., NH), 2207 (2CN), 1630 (CO); ^{1}H NMR (DMSO) δ = 2.19 (s, 3H, CH_3), 5.54 (s, 1H, pyrimidine-H), 7.28 (d, 1H, J = 5.1 Hz, Ar), 7.82 (dd, 1H, J = 3 Hz, Ar), 8.00 (d, 1H, J = 5.1 Hz, Ar), 8.32 (s, 1H, CH), 10.84 (s, 1H, NH); m/z = 307 (M^+, 64.8%), 278 (15.7%), 251 (8.4%), 213 (8.4%), 149 (4.5%), 113 (17.8%), 98 (19.0%), 84 (93.1%), 71 (36.3%), 57 (100%); Anal. Calcd for $C_{15}H_9N_5OS$: C, 58.62; H, 2.95; N, 22.79; S, 10.43. Found: C, 58.82; H, 2.77; N, 22.49; S, 10.63%.

4.1.4.7. 2-(1-Cyano-2-(2,5-dimethoxyphenyl)vinyl)-5-methyl-7-oxo-4,7-dihydropyra-zolo[1,5-a]pyrimidine-3-carbonitrile ***7j***. Brown crystals, yield 64%, m.p > 300 °C, ν_{max}/cm^{-1} (KBr) 3414 (br., NH), 2214 (2CN), 1630 (CO); ^{1}H NMR (DMSO) δ = 2.49 (s, 3H, CH_3), 3.84 (s, 3H, OCH_3), 3.87 (s, 3H, OCH_3), 5.74 (s, 1H, pyrimidine-H), 7.14–7.71 (m, 3H, Ar), 8.44 (s, 1H, CH), 10.48 (s, 1H, NH); m/z = 362 (M^+ + 1, 0.3%), 305 (2.1%), 279 (1.8%), 259 (4.0%), 247 (3.6%), 213 (1.5%), 189 (4.3%), 149 (16.3%), 113 (28.9%), 87 (26.6%), 71 (29.8%), 59 (100%); Anal. Calcd for $C_{19}H_{15}N_5O_3$: C, 63.15; H, 4.18; N, 19.38. Found: C, 63.32; H, 4.05; N, 19.59%.

4.1.4.8. 2-(1-Cyano-2-(3,4,5-trimethoxyphenyl)vinyl)-5-methyl-7-oxo-4,7-dihydropyr-azolo[1,5-a]pyrimidine-3-carbonitrile ***7h***. Brown crystals, yield 57%, m.p > 300 °C, ν_{max}/cm^{-1} (KBr) 3190 (NH), 2222 (2CN), 1635 (CO); ^{1}H NMR (DMSO) δ = 2.49 (s, 3H, CH_3), 3.76 (s, 3H, OCH_3), 3.82 (s, 6H, 2OCH_3), 5.78 (s, 1H, pyrimidine-H), 7.29 (s, 2H, Ar), 8.02 (s, 1H, CH), 9.97 (s, 1H, NH); Anal. Calcd for $C_{20}H_{17}N_5O_4$: C, 61.38; H, 4.38; N, 17.89. Found: C, 61.57; H, 4.55; N, 17.64%.

4.1.4.9. 2-(1-Cyano-2-(4-hydroxy-3-methoxyphenyl)vinyl)-5-methyl-7-oxo-4,7-dihydropyrazolo[1,5-a]pyrimidine-3-carbonitrile ***7i***. Brown crystals, yield 61%, m.p > 300 °C, ν_{max}/cm^{-1} (KBr) 3170 (NH), 2211 (2CN), 1629 (CO); ^{1}H NMR (DMSO) δ = 2.49 (s, 3H, CH_3), 3.84 (s, 3H, OCH_3), 5.77 (s, 1H, pyrimidine-H), 6.93 (s, 1H, Ar), 7.39–7.67 (m, 2H, Ar), 7.94 (s, 1H, CH), 9.74 (s, 1H, OH), 9.92 (s, 1H, NH); m/z = 347 (M^+, 0.5%), 305 (2.3%), 277 (2.5%), 259 (4.6%), 247 (4.4%), 213 (1.6%), 189 (6.0%), 167 (3.7%), 113 (38.4%), 87 (31.3%), 71 (28.0%), 59 (100%); Anal. Calcd for $C_{18}H_{13}N_5O_3$: C, 62.24; H, 3.77; N, 20.16. Found: C, 62.40; H, 3.61; N, 20.46%.

4.1.5. General procedure for preparation of compounds ***10a,b***

To a solution of **5** (0.01 mol) was added the appropriate *o*-hydroxybenzaldehydes **8a, b** (0.01 mol) in *N,N*-dimethylformamide (10 ml) containing few drops of piperidine under was refluxed for 4 h. The solid product so formed was collected by filtration, washed with ethanol and recrystallized from an ethanol-dioxane mixture to give the respective products **10a,b**.

4.1.5.1. 2-(2-Imino-2H-chromen-3-yl)-5-methyl-7-oxo-4,7-dihydropyrazolo[1,5-a]-pyrimidine-3-carbonitrile ***10a***. Reddish brown crystals, yield 74%, m.p > 300 °C, ν_{max}/cm^{-1} (KBr) 3431 (2NH), 2212 (CN), 1628 (CO); ^{1}H NMR (DMSO) δ = 2.49 (s, 3H, CH_3), 5.81 (s, 1H, pyrimidine-H), 7.10–8.62 (m, 5H, Ar), 9.11 (s, 1H, NH), 10.21 (s, 1H, NH); Anal. Calcd for $C_{17}H_{11}N_5O_2$: C, 64.35; H, 3.49; N, 22.07. Found: C, 64.52; H, 3.34; N, 22.27%.

4.1.5.2. 2-(7-Hydroxy-2-imino-2H-chromen-3-yl)-5-methyl-7-oxo-4,7-dihydropyra-zolo[1,5-a]pyrimidine-3-carbonitrile ***10b***. Reddish brown crystals, yield 56%, m.p > 300 °C, ν_{max}/cm^{-1} (KBr) 3423 (OH), 3187 (2NH), 2211 (CN), 1626 (CO); ^{1}H NMR (DMSO) δ = 2.49 (s, 3H, CH_3), 5.62 (s, 1H, pyrimidine-H), 6.61–7.90 (m, 4H, Ar), 8.72 (s, 1H, NH), 9.74 (s, 1H, NH), 8.82 (s, 1H, OH); Anal. Calcd for $C_{17}H_{11}N_5O_3$: C, 61.26; H, 3.33; N, 21.01. Found: C, 61.41; H, 3.16; N, 21.24%.

4.1.6. General procedure for preparation of compounds ***11a,b***

Compounds **10a,b** (0.01 mol) were refluxed in sodium ethoxide solution [prepared as usual by dissolving sodium metal (0.01 mol) in absolute ethanol (15 ml)] for 5 h. The solid product so formed was filtered off, washed with ethanol and recrystallized from an ethanol-dioxane mixture to give the respective products **11a,b**.

4.1.6.1. 5-Imino-3-methyl-4,5-dihydro-1H-chromeno[3″,2″:5′,6′]pyrido[4′,3′:3,4]-pyrazolo[1,5-a]pyrimidin-1-one ***11a***. Brown crystals, yield 55%, m.p > 300 °C, ν_{max}/cm^{-1} (KBr) 3431 (NH), 3209 (NH), 1633 (CO); ^{1}H NMR (DMSO) δ = 2.32 (s, 3H, CH_3), 5.74 (s, 1H, pyrimidine-H), 6.92–8.21 (m, 5H, Ar), 9.23 (s, 1H, NH), 9.41 (s, 1H, NH); Anal. Calcd for $C_{17}H_{11}N_5O_2$: C, 64.35; H, 3.49; N, 22.07. Found: C, 64.50; H, 3.37; N, 22.29%.

4.1.6.2. 9-Hydroxy-5-imino-3-methyl-4,5-dihydro-1H-chromeno[3″,2″:5′,6′]pyrido-[4′,3′:3,4]pyrazolo[1,5-a]pyrimidin-1-one ***11b***. Brown crystals, yield 72%, m.p > 300 °C, ν_{max}/cm^{-1} (KBr) 3423 (OH), 3321 (2NH), 1633 (CO); ^{1}H NMR (DMSO) δ = 2.42 (s, 3H, CH_3), 5.62 (s, 1H, pyrimidine-H), 6.61–7.90 (m, 4H, Ar), 8.41 (s, 1H, NH), 8.79 (s, 1H, NH), 8.86 (s, 1H, OH); Anal. Calcd for $C_{17}H_{11}N_5O_3$: C, 61.26; H, 3.33; N, 21.01. Found: C, 61.11; H, 3.50; N, 21.26%.

4.1.7. 2-(2-Imino-2,4a-dihydropyrano[2,3-b]indol-3-yl)-5-methyl-7-oxo-4,7-dihydro-pyrazolo[1,5-a]pyrimidine-3-carbonitrile ***14***

A mixture of compound **5** (0.01 mol) and indoline-2,3-dione **12** (0.01 mol) in *N*, *N*- dimethylformamide (10 ml) containing few drops of piperidine was refluxed for 4 h. The solid product so formed was collected by filtration, washed with ethanol and recrystallized from an ethanol-dioxane mixture to give the respective product**14**.Brown crystals, yield 70%, m.p > 300 °C, ν_{max}/cm^{-1} (KBr) 3418 (NH), 3209 (NH), 2214 (CN), 1656 (CO); ^{1}H NMR (DMSO) δ = 2.48 (s, 3H, CH_3), 5.72 (s, 1H, pyrimidine-H), 6.81–8.22 (m, 5H, Ar), 8.42 (s, 1H, NH), 8.62 (s, 1H, NH); Anal. Calcd for $C_{19}H_{12}N_6O_2$: C, 64.04; H, 3.39; N,

23.58. Found: C, 64.21; H, 3.25; N, 23.37%.

*4.1.8. 5-Imino-3-methyl-5,12b-dihydropyrimido[1‴,2‴:1″,5″]pyrazolo [3″,4″:-4′,5′]-pyrido[3′,2′:5,6]pyrano[2,3-b]indol-1(4H)-one **15***

Compound **14** (0.01 mol) was refluxed in sodium ethoxide solution [prepared as usual by dissolving sodium metal (0.01 mol) in absolute ethanol (15 ml)] for 5 h. The solid product so formed was filtered off, washed with ethanol and recrystallized from an ethanol-dioxane mixture to give the respective products **15**. Brown crystals, yield 70%, m.p > 300 °C, ν_{max}/cm^{-1} (KBr) 3425 (br, 2NH), 1650 (CO); ^{1}H NMR (DMSO) δ = 2.31 (s, 3H, CH_3), 5.66 (s, 1H, pyrimidine-H), 6.22–8.21 (m, 5H, Ar), 8.52 (s, 1H, NH), 8.61 (s, 1H, NH); Anal. Calcd for $C_{19}H_{12}N_6O_2$: C, 64.04; H, 3.39; N, 23.58. Found: C, 64.23; H, 3.25; N, 23.35%.

*4.1.9. General procedure for preparation compounds **18a-d***

A mixture of **5** (0.01 mol) and 4-arylazosalicylaldehyde derivatives **16a-d** (0.01 mol) in *N*,*N*-dimethylformamide (10 ml) with few drops of piperidine was refluxed for 4 h. The solid product so formed was collected by filtration, washed with ethanol and recrystallized from an ethanol-dioxane mixture to give the respective products **18a-d**.

*4.1.9.1. 2-(2-Imino-6-(phenyldiazenyl)-2H-chromen-3-yl)-5-methyl-7-oxo-4,7-dihydropyrazolo[1,5-a]pyrimidine-3-carbonitrile **18a***. Reddish brown crystals, yield 65%, m.p > 300 °C, ν_{max}/cm^{-1} (KBr) 3416 (br., NH), 2210 (CN), 1602 (CO); ^{1}HNMR (DMSO) δ = 2.32 (s, 3H, CH_3), 5.76 (s, 1H, pyrimidine-H), 7.41–8.10 (m, 9H, Ar), 9.11 (s, 1H, NH), 9.32 (s, 1H, NH); Anal. Calcd for $C_{23}H_{15}N_7O_2$: C, 65.55; H, 3.59; N, 23.27. Found: C, 65.40; H, 3.42; N, 23.48%.

*4.1.9.2. 2-(2-Imino-6-(p-tolyldiazenyl)-2H-chromen-3-yl)-5-methyl-7-oxo-4,7-dihydropyrazolo[1,5-a]pyrimidine-3-carbonitrile **18b***. Reddish brown crystals, yield 84%, m.p > 300 °C, ν_{max}/cm^{-1} (KBr) 3417 (br., NH), 2213 (CN), 1622 (CO); ^{1}HNMR (DMSO) δ = 2.34 (s, 3H, CH_3), 2.39 (s, 3H, CH_3), 5.81 (s, 1H, pyrimidine-H), 7.29–7.95 (m, 8H, Ar), 9.21 (s, 1H, NH), 9.25 (s, 1H, NH); Anal. Calcd for $C_{24}H_{17}N_7O_2$: C, 66.20; H, 3.94; N, 22.52. Found: C, 66.03; H, 3.75; N, 22.68%.

*4.1.9.3. 2-(2-Imino-6-((4-methoxyphenyl)diazenyl)-2H-chromen-3-yl)-5-methyl-7-oxo-4,7-dihydropyrazolo[1,5-a]pyrimidine-3-carbonitrile **18c***. Brown crystals, yield 71%, m.p > 300 °C, ν_{max}/cm^{-1} (KBr) 3376 (br., NH), 2212 (CN), 1600 (CO); ^{1}HNMR (DMSO) δ = 2.34 (s, 3H, CH_3), 3.84 (s, 3H, OCH_3), 5.84 (s, 1H, pyrimidine-H), 7.06–7.94 (m, 8H, Ar), 9.23 (s, 1H, NH), 9.31 (s, 1H, NH); Anal. Calcd for $C_{24}H_{17}N_7O_3$: C, 63.85; H, 3.80; N, 21.72. Found: C, 63.68; H, 3.63; N, 21.50%.

*4.1.9.4. 2-(6-((4-Chlorophenyl)diazenyl)-2-imino-2H-chromen-3-yl)-5-methyl-7-oxo-4,7-dihydropyrazolo[1,5-a]pyrimidine-3-carbonitrile **18d***. Reddish brown crystals, yield 76%, m.p > 300 °C, ν_{max}/cm^{-1} (KBr) 3420 (br., NH), 2212 (CN), 1630 (CO); ^{1}HNMR (DMSO) δ = 2.21 (s, 3H, CH_3), 5.68 (s, 1H, pyrimidine-H), 7.05–8.01 (m, 8H, Ar), 9.11 (s, 1H, NH), 9.23 (s, 1H, NH); Anal. Calcd for $C_{23}H_{14}ClN_7O_2$: C, 60.60; H, 3.10; Cl, 7.78; N, 21.51. Found: C, 60.75; H, 3.27; N, 21.30%.

*4.1.10. General procedure for preparation of compounds **19a-d***

Compounds **18a-d** (0.01 mol) were refluxed in sodium ethoxide solution (15 ml) for 4 h. The solid so formed was filtered off, washed with ethanol and recrystallized from acetic acid mixture to give the respective products **19a-d**.

*4.1.10.1. 5-Imino-3-methyl-10-(phenyldiazenyl)-4,5-dihydro-1H-chromeno[3″,2″:-5′,6′]pyrido[4′,3′:3,4]pyrazolo[1,5-a]pyrimidin-1-one **19a***. Brown crystals, yield 84%, m.p > 300 °C, ν_{max}/cm^{-1} (KBr) 3416 (br., NH), 1602 (CO); ^{1}HNMR (DMSO) δ = 2.34 (s, 3H, CH_3), 5.68 (s, 1H, pyrimidine-H), 7.43–7.98 (m, 9H, Ar), 9.12 (s, 1H, NH), 9.36 (s, 1H, NH); Anal. Calcd for $C_{23}H_{15}N_7O_2$: C, 65.55; H, 3.59; N, 23.27. Found: C, 65.42; H, 3.41; N, 23.49%.

*4.1.10.2. 5-Imino-3-methyl-10-(p-tolyldiazenyl)-4,5-dihydro-1H-chromeno[3″,2″:-5′,6′]-pyrido[4′,3′:3,4]pyrazolo[1,5-a]pyrimidin-1-one **19b***. Brown crystals, yield 70%, m.p > 300 °C, ν_{max}/cm^{-1} (KBr) 3420 (br., NH), 1630 (CO); ^{1}HNMR (DMSO) δ = 2.22 (s, 3H, CH_3), 2.34 (s, 3H, CH_3), 5.84 (s, 1H, pyrimidine-H), 7.21–8.11 (m, 8H, Ar), 9.22 (s, 1H, NH), 9.28 (s, 1H, NH); Anal. Calcd for $C_{24}H_{17}N_7O_2$: C, 66.20; H, 3.94; N, 22.52. Found: C, 66.37; H, 3.78; N, 22.72%.

*4.1.10.3. 5-Imino-10-((4-methoxyphenyl)diazenyl)-3-methyl-4,5-dihydro-1H-chromeno[3″,2″:5′,6′]pyrido[4′,3′:3,4]pyrazolo[1,5-a]pyrimidin-1-one **19c***. Brown crystals, yield 76%, m.p > 300 °C, ν_{max}/cm^{-1} (KBr) 3370 (NH), 3180 (NH), 1620 (CO); ^{1}HNMR (DMSO) δ = 2.24 (s, 3H, CH_3), 3.80 (s, 3H, OCH_3), 5.74 (s, 1H, pyrimidine-H), 7.05–7.98 (m, 8H, Ar), 9.02 (s, 1H, NH), 9.32 (s, 1H, NH); Anal. Calcd for $C_{24}H_{17}N_7O_3$: C, 63.85; H, 3.80; N, 21.72. Found: C, 63.64; H, 3.65; N, 21.52%.

*4.1.10.4. 10-((4-Chlorophenyl)diazenyl)-5-imino-3-methyl-4,5-dihydro-1H-chromeno-[3″,2″:5′,6′]pyrido[4′,3′:3,4]pyrazolo[1,5-a]pyrimidin-1-one **19d***. Brown crystals, yield 66%, m.p > 300 °C, ν_{max}/cm^{-1} (KBr) 3440 (br., NH), 1656 (CO); ^{1}HNMR (DMSO) δ = 2.31 (s, 3H, CH_3), 5.81 (s, 1H, pyrimidine-H), 7.11–7.99 (m, 8H, Ar), 9.12 (s, 1H, NH), 9.19 (s, 1H, NH); Anal. Calcd for $C_{23}H_{14}ClN_7O_2$: C, 60.60; H, 3.10; Cl, 7.78; N, 21.51. Found: C, 60.77; H, 3.25; N, 21.31%.

*4.1.11. General procedure for preparation of compounds **21a-d***

A solution of compound **5** (0.01 mol) in *N*, *N*-dimethylformamide and sodium hydroxide was cooled in an ice bath at (0–5 °C) while being stirred. To the resulting cold solution was added portion wise a cold solution of the appropriate arenediazonium salt, prepared as usual by diazotizing the corresponding aromatic amine **20** (0.01 mol) in concentrated hydrochloric acid (3 ml) with sodium nitrite (0.01 mol) in water (3 ml). After all diazonium salt solution was added, the mixture was stirred for further 1 h, while cooling in an ice-bath. The solid that precipitated was filtered off, washed with water, dried and finally recrystallized from an ethanol-dioxane mixture to give products **21a-d**. The physical constants and spectral data are shown below:

*4.1.11.1. 3-Cyano-5-methyl-7-oxo-N-phenyl-4,7-dihydropyrazolo[1,5-a] pyrimidine-2-carbohydrazonoyl cyanide **21a***. Reddish brown crystals, yield 76%, m.p > 300 °C, ν_{max}/cm^{-1} (KBr) 3411 (NH), 3152 (NH), 2224 (2CN), 1669 (CO); ^{1}HNMR (DMSO) δ = 2.31 (s, 3H, CH_3), 5.85 (s, 1H, pyrimidine-H), 6.92–7.94 (m, 5H, Ar), 10.31 (s, 1H, NH), 13.4 (s, 1H, NH); Anal. Calcd for $C_{16}H_{11}N_7O$: C, 60.56; H, 3.49; N, 30.90. Found: C, 60.73; H, 3.33; N, 30.69%.

*4.1.11.2. 3-Cyano-5-methyl-7-oxo-N-(p-tolyl)-4,7-dihydropyrazolo[1,5-a] pyrimidine-2-carbohydrazonoyl cyanide **21b***. Brown crystals, yield 60%, m.p > 300 °C, ν_{max}/cm^{-1} (KBr) 3323 (NH), 3172 (NH), 2216 (2CN), 1636 (CO);^{1}H NMR (DMSO) δ = 2.29 (s, 3H, CH_3), 2.32 (s, 3H, CH_3), 5.81 (s, 1H, pyrimidine-H), 7.15 (d, 2H, *J* = 7.8 Hz, Ar), 7.51 (d, 2H, *J* = 8.1 Hz, Ar), 10.23 (s, 1H, NH), 12.11 (s, 1H, NH); Anal. Calcd for $C_{17}H_{13}N_7O$: C, 61.62; H, 3.95; N, 29.59. Found: C, 61.47; H, 3.78; N, 29.79%.

*4.1.11.3. 3-Cyano-N-(4-methoxyphenyl)-5-methyl-7-oxo-4,7-dihydropyrazolo[1,5-a]-pyrimidine-2-carbohydrazonoyl cyanide **21c***. Brown crystals, yield 607%, m.p > 300 °C, ν_{max}/cm^{-1} (KBr) 3430 (br., 2NH), 2227 (2CN), 1622 (CO);^{1}H NMR (DMSO) δ = 2.24 (s, 3H, CH_3), 3.81 (s, 3H, OCH_3),5.76 (s, 1H, pyrimidine-H), 7.41 (d, 2H, *J* = 8.1 Hz, Ar), 7.50 (d, 2H, *J* = 8.4 Hz, Ar), 10.11 (s, 1H, NH), 12.09 (s, 1H, NH); Anal. Calcd for $C_{17}H_{13}N_7O_2$: C, 58.79; H, 3.77; N, 28.23. Found: C, 58.64; H, 3.60; N, 28.43%.

*4.1.11.4. N-(4-Chlorophenyl)-3-cyano-5-methyl-7-oxo-4,7-dihydropyrazolo [1,5-a]-pyrimidine-2-carbohydrazonoyl cyanide **21d***. Brown crystals, yield 60%, m.p > 300 °C, ν_{max}/cm^{-1} (KBr) 3424 (br., 2NH), 2216 (2CN),

1635 (CO); ^{1}H NMR (DMSO) δ = 2.29 (s, 3H, CH_3), 5.76 (s, 1H, pyrimidine-H), 6.57 (d, 2H, J = 7.8 Hz, Ar), 6.98 (d, 2H, J = 8.1 Hz, Ar), 10.21 (s, 1H, NH), 12.81 (s, 1H, NH); m/z = 353 (M^{+2}, 1.5%), 327 (1.2%), 294 (45.5%), 266 (21.6%), 213 (3.4%), 174 (6.9%), 147 (11.9%), 111 (23.4%), 85 (34.5%), 71 (56.3%), 57 (100%); Anal. Calcd for $C_{16}H_{10}ClN_7O$: C, 54.63; H, 2.87; Cl, 10.08; N, 27.87. Found: C, 54.50; H, 2.71; N, 27.69%.

4.2. Biological study

4.2.1. Materials and methods

4.2.1.1. Cell line. Two human tumor cell line namely: Mammary gland (MCF-7) and Epitheliod Carcinoma (HeLa). The cell lines were obtained from ATCC *via* Holding company for biological products and vaccines (VACSERA), Cairo, Egypt.

Doxorubicin was used as a standard anticancer drug for comparison.

4.2.1.2. Chemical reagents. The reagents RPMI-1640 medium, MTT and DMSO (sigma co., St. Louis, USA), Fetal Bovine serum (GIBCO, UK)

4.2.1.3. MTT assay. The cell lines mentioned above were used to determine the inhibitory effects of compounds on cell growth using the MTT assay [38,39]. This colorimetric assay is based on the conversion of the yellow tetrazolium bromide (MTT) to a purple formazan derivative by mitochondrial succinate dehydrogenase in viable cells. Cell lines were cultured in RPMI-1640 medium with 10% fetal bovine serum. Antibiotics added were 100 units/ml penicillin and 100 µg/ml streptomycin at 37 °C in a 5% CO_2 incubator. The cell lines were seeded in a 96-well plate at a density of 1.0x10^4 cells/well at 37 °C for 48 h under 5% CO_2. After incubation the cells were treated with different concentration of compounds and incubated for 24 h. After 24 h of drug treatment, 20 µl of MTT solution at 5 mg/ml was added and incubated for 4 h. Dimethyl sulfoxide (DMSO) in volume of 100 µl is added into each well to dissolve the purple formazan formed. The colorimetric assay is measured and recorded at absorbance of 570 nm using a plate reader (EXL 800, USA). The relative cell viability in percentage was calculated as (A570 of treated samples/A570 of untreated sample) × 100. Triplicate well plates were prepared for each individual dose.

4.2.2. Statistical evaluation

Results obtained as mean ± SD (standard deviation).

4.2.3. KDM (Histone lysine demethylases) inhibitory assay

The in *vitro* inhibitory activities of the synthesized compounds **5**, **7e** and **7i** against KDM were carried out using ELISA assay. KMD and ATP were purchased from Sigma. First, the KDMs were incubated with the synthesized compounds in enzymatic buffer for 5 min in order to start the enzymatic reaction, ATP (1.65 µM) was added into the reaction mixture. The assay were conducted for 30 min at room temperature. The reaction was stopped by addition of detection reagents which contain EDTA. The detection step continued for 1 h, then the IC_{50} values were determined by GraphPad Prism 5.0. Three independent experiments were performed for each concentration.

4.2.4. In-vitro DNA-flow cytometric (cell cycle) analysis

MCF-7 cells were exposed to the most active member **7e** for 48 h. Then, the tested cells were collected by trypsinization and washed in PBS. Ice-cold absolute ethanol was used for fixation of the collected cells. The cells were stained with Cycle TESTTM PLUS DNA Reagent Kit (BD Biosciences, San Jose, CA) according to the manufacturer's instructions. Cell cycle distribution was evaluated using a flowcytometer.

4.2.5. Annexin V-FITC apoptosis assay

As described above, MCF-7 cells were seeded and incubated with compound **7e** for 48 h. Then, the cells were collected and washed with PBS two successive times. The cells were exposed to centrifugation. Thereafter, the cells were treated with Annexin V-FITC and propidium iodide (PI) using the apoptosis detection kit (BD Biosciences, San Jose, CA) according to the manufacturer's protocol. Annexin V-FITC and PI binding were analyzed by a flowcytometer.

4.3. Modeling studies

4.3.1. Molecular docking study

Docking studies and all modeling calculations were performed using program "Molecular Operating Environment (MOE) version 2009.10 [40]. KDM5A structure was downloaded from the PDB data bank (http://www.rcsb.org/PDB codes: 5IVE). The protein was prepared according to the following:

(i) Removal of target compounds from the enzyme active site.
(ii) Hydrogen atoms were added to the proteins with MOE and minimized keeping all the heavy atoms fixed until RMS gradient of 0.01 kcal mol^{-1}, and RMS distance of 0.1 Å were reached.
(iii) Partial charges were computed using MMFF94x force field.
(iv) The ligands were built employing the MOE builder interface.
(v) The structures were subjected to energy minimization and the partial charges were computed using MMFF94x force field.
(vi) Docking calculations were done using Alpha triangle placement method and poses were prioritized by London dG scoring method.

Appendix A. Supplementary material

Supplementary data to this article can be found online at https://doi.org/10.1016/j.bioorg.2019.102929.

References

[1] K. Nepali, S. Sharma, M. Sharma, P.M. Bedi, K.L. Dhar, Rational approaches, design strategies, structure activity relationship and mechanistic insights for anticancer hybrids, Eur. J. Med. Chem. 77 (2014) 422–487.
[2] U.S. Rai, A.M. Isloor, P. Shetty, K.S.R. Pai, H.K. Fun, Synthesis and in vitro biological evaluation of new pyrazole chalcones and heterocyclic diamides as potential anticancer agents, Arab. J. Chem. 8 (2015) 317–321.
[3] L. Livraghi, J.E. Garber, PARP inhibitors in the management of breast cancer: current data and future prospects, BMC Med. 13 (2015) 188.
[4] E.L. Mayer, Targeting breast cancer with CDK inhibitors, Curr. Oncol. Rep. 17 (2015) 20.
[5] L.C. Young, M.J. Hendzel, The oncogenic potential of Jumonji D2 (JMJD2/KDM4) histone demethylase overexpression, Biochem. Cell Biol. 91 (2013) 369–377.
[6] R. Bhattacharya, N. Kang-Decker, D.A. Hughes, P. Mukherjee, V. Shah, M.A.M. Niven, D. Mukhopadhyay, Regulatory role of dynamin-2 in vegfr-2/kdr-mediated endothelial signaling, FASEB J. 19 (2005) 1692–1694.
[7] S. Wee, D. Dhanak, H. Li, S.A. Armstrong, R.A. Copeland, R. Sims, S.B. Baylin, X.S. Liu, L. Schweizer, Targeting epigenetic regulators for cancer therapy New York, Ann., Acad. Sci. 30 (2014).
[8] W.J. HØjfeldt, K. Agger, K. Helin, Histone lysine demethylases as targets for anticancer therapy, Nat. Rev. Drug Disc. 12 (2013) 917.
[9] J. McGrath, P. Trojer, Targeting histone lysine methylation in cancer, Pharmacol. Ther. 150 (2015) 1–22.
[10] Y. Shi, F. Lan, C. Matson, J.R. Whetstine, P.A. Cole, R.A. Casero, Y. Shi, Histone demethylation mediated by the nuclear amine oxidase homolog LSD1, Cell 119 (2004) 941–953.
[11] M. Katoh, M. Katoh, Identification and characterization of JMJD2 family genes in silico, Int. J. Oncol. 24 (2004) 1623–1628.
[12] P.B. Rasmussen, P. Staller, The KDM5 family of histone demethylases as targets in oncology drug discovery, Epgienomics 6 (2014) 277–286.
[13] Y. Li, W. Gao, F. Li, J. Wang, J. Zhang, Y. Yang, S. Zhang, L. Yang, An in silicoexploration of the interaction mechanism of pyrazolo[1,5-*a*]pyrimidine type CDK2inhibitors, Mol. Biosyst. 9 (2013) 2266–2281.
[14] J.Y. Hwang, M.P. Windisch, S. Jo, K. Kim, S. Kong, H.C. Kim, S. Kim, H. Kim, M.E. Lee, Y. Kim, J. Choi, D. Park, E. Park, J. Kwon, J. Nam, S. Ahn, J. Cechetto, J. Kim, M. Liuzzi, Z. No, J. Lee, Discovery and characterization of a novel 7-aminopyrazolo[1,5-*a*]pyrimidine analog as a potent hepatitis C virus inhibitor, Bioorg. Med. Chem. Lett. 22 (2012) 7297–7301.
[15] S. Selleri, F. Bruni, C. Costagli, A. Costanzo, G. Guerrini, G. Ciciani, P. Gratteri, F. Besnard, B. Costa, M. Montali, C. Martini, J. Fohlin, G.D. Siena, P.M. Aiello, A novel selective GABAA *α*1 receptor agonist displaying sedative and anxiolytic-like properties in rodents, J. Med. Chem. 48 (2005) 6756–6760.
[16] J. Xu, H. Liu, G. Li, Y. He, R. Ding, X. Wang, M. Feng, S. Zhang, Y. Chen, S. Li, M. Zhao, Y. Li, C. Qi, Synthesis and biological evaluation of 7-(2-

chlorophenylamino)-5-((2-[18F]fluoro-ethyoxy)methyl)pyrazolo[1,5-*a*]pyrimidine-3-carbonitrile as PET tumor imaging agent, Z. Naturforsch. B. Chem. Sci. 67 (2012) 827–834.
[17] Y. Tian, D. Du, D. Rai, L. Wang, H. Liu, P. Zhan, E.D. Clercq, C. Pannecouque, X. Liu, Fused heterocyclic compounds bearing bridgehead nitrogen as potent HIV-1 NNRTIs. Part 1: Design, synthesis and biological evaluation of novel 5,7-disubstituted pyrazolo[1,5-*a*]pyrimidine derivatives, Bioorg. Med. Chem. 22 (2014) 2052–2059.
[18] E.J. Hanan, A.V. Abbema, K. Barrett, W.S. Blair, J. Blaney, C. Chang, C. Eigenbrot, S. Flynn, P. Gibbons, C.A. Hurley, J.R. Kenny, J. Kulagowski, L. Lee, S.R. Magnuson, C. Morris, J. Murray, R.M. Pastor, T. Rawson, M. Siu, M. Ultsch, A. Zhou, D. Sampath, J.P. Lyssikatos, Discovery of potent and selective pyrazolopyrimidine Janus kinase 2 inhibitors, J. Med. Chem. 55 (2012) 10090–10107.
[19] P. Kaswan, K. Pericherla, D. Purohit, A. Kumar, Synthesis of 5,7-diarylpyrazolo[1,5-*a*]pyrimidines *via* KOH mediated tandem reaction of 1*H*-pyrazol-3-amines and chalcones, Tetrahedron Lett. 56 (2015) 549–553.
[20] M. Drev, U. Groselj, S. Mevec, E. Pusavec, J. Strekelj, A. Golobic, G. Dahmann, B. Stanovnik, J. Svete, Regioselective synthesis of 1- and 4-substituted 7-oxopyrazolo[1,5-*a*]pyrimidine-3-carboxamides, Tetrahedron 70 (2014) 8267–8279.
[21] P.B. Yu, C.C. Hong, C. Sachidanandan, J.L. Babitt, D.Y. Deng, S.A. Hoyng, H.Y. Lin, K.D. Bloch, R.T. Peterson, Dorsomorphin inhibits BMP signals required for embryogenesis and iron metabolism, Nat. Chem. Biol. 4 (2008) 33–41.
[22] N. Kato, M. Oka, T. Murase, M. Yoshida, M. Sakairi, S. Yamashita, Y. Yasuda, A. Yoshikawa, Y. Hayashi, M. Makino, M. Takeda, Y. Mirensha, T. Kakigami, Discovery and pharmacological characterization of *N*-[2-({2-[(2*S*)-2-cyanopyrrolidin-1-yl]-2-oxoethyl}amino)-2-methylpropyl]-2-methylpyrazolo[1,5-*a*]pyrimidine-6-carboxamide hydrochloride (anagliptin hydrochloride salt) as a potent and selective DPP-IV inhibitor, Bioorg. Med. Chem. 19 (2011) 7221–7227.
[23] A.S. Hassan, T.S. Hafez, S.A. Osman, Synthesis, characterization and cytotoxicity of some new 5-aminopyrazole and pyrazolo[1,5-*a*]pyrimidine derivatives, Sci. Pharm. 83 (2015) 27–39.
[24] M. Gale, J. Sayegh, J. Cao, M. Norcia, P. Gareiss, D. Hoyer, J.S. Merkel, Q. Yan, Screen-identified selective inhibitor of lysine demethylase 5A blocks cancer cell growth and drug resistance, Oncotarget 7 (2016) 39931–39944.
[25] V.S. Gehling, S.F. Bellon, J.C. Harmange, Y. LeBlanc, F. Poy, S. Odate, S. Buker, F. Lan, S. Arora, K.E. Williamson, P. Sandy, R.T. Cumming, C.M. Bailey, L. Berqeron, W. Mao, A. Gustafson, Y. Liu, P.E. Vander, J.E. Audia, P. Trojer, B.K. Albrecht, Identification of potent, selective KDM5 inhibitors, Bioorg. Med. Chem. Lett. 26 (2016) 4350–4354.
[26] N.H. Metwally, M.A. Badawy, D.S. Okpy, Synthesis and anticancer activity of some new thiopyrano[2,3-*d*]thiazoles incorporating pyrazole moiety, Chem. Pharm. Bull. 63 (2015) 495–503.
[27] N.H. Metwally, F.M. Abdelrazek, S.M. Eldaly, Synthesis and anticancer activity of some new heterocyclic compounds based on 1-cyanoacetyl-3,5-dimethylpyrazole, Res. Chem. Intermed. 42 (2016) 1071–1089.
[28] N.H. Metwally, E.A. Deeb, Synthesis, assessment on human breast, liver and colon cell lines and molecular modeling study using novel pyrazolo[4,3-c]pyridine derivatives, Bioorg. Chem. 77 (2018) 203–214.
[29] N.H. Metwally, F.M. Abdelrazek, S.M. Eldaly, Synthesis, molecular docking, and biological evalutaion of some novel bis-heterocyclic compounds based N, N-([1,1'biphenyldiyl])bis(2-cyanoacetamide) as potential anticancer agents, J. Heter. Chem. 55 (2018) 2668–2682.
[30] N.H. Metwally, I.T. Radwan, W.S. El-Serwy, M.A. Mohamed, Design, synthesis, DNA assessment amd molecular docking study of novel 2-(pyridine-2-ylimino)thiazolidin-4-one derivatives as potent antifungal agents, Bioorg. Chem. 84 (2019) 456–467.
[31] A.S. Shawali, N.M.S. Harb, K.O.A. Badhdah, study of tautomerism in diazonium coupling products of 4-hydroxycoumarin, J. Heterocycl. Chem. 22 (1985) 1397–1403.
[32] R. Joneo, A.J. Ryan, S. Stemhell, S.E. Wrifgt, The structures of some-5-pyrazolone and derived 4-arylazo-5-pyrazolones, Tetrahedron 19 (1963) 1497–1507.
[33] S.A. Shawali, H.A. Albar, Kinetics and mechanism of dehydrochlorination of *N*-aryl-C ethoxycarbonylformohydrazidoyl chlorides, Can. J. Chem. 64 (1986) 871–875.
[34] A.M. Rieger, K.L. Nelson, J.D. Konowalchuk, D.R. Barreda, Modified Annexin VI propidium iodide apoptosis assay for accurate assessment of cell death, J. Vis. Exp. 50 (2011) 2597.
[35] L.Z. Benet, C.M. Hosey, O. Ursu, T. Oprea, BDDCS, the rule of 5 and drugability, Adv. Drug Deliv. Rev. 101 (2016) 89–98.
[36] H. Pajouhesh, G.R. Lenz, Medicinal chemical properties of successful central nervous system drugs, J. Am. Soc. Exp. Neurother. 2 (2005) 541–553.
[37] R.A. Carboni, D.D. Coffman, E.G. Howard, Cyanocarbon chemistry. XI.1 malononitrile dimer, J. Amer. Chem. Soc. 80 (1958) 2838–2840.
[38] T. Mosmann, Rapid colorimetric assay for cellular growth and survival: application to proliferation and cytotoxicity assays, Immunol. Methods 65 (1983) 55–63.
[39] F. Denizot, R. Lang, Rapid colorimetric assay for cell growth and survival. Modifications to the tetrazolium dye procedure giving improved sensitivity and reliability, J. Immunol. Methods 22 (1986) 271–277.
[40] C.C. Group, Chemical Computing Group and Molecular Network Announce the integration of CORINA into MOE, 2007.